La investigación reportada en esta tesis es parte de los programas de investigación del CICESE (Centro de Investigación Científica y de Educación Superior de Ensenada, Baja California).

La investigación fue financiada por el CONAHCYT (Consejo Nacional de Humanidades, Ciencias y Tecnologías).

Centro de Investigación Científica y de Educación Superior de Ensenada, Baja California

Doctor of Science in Marine Ecology

Flocculation of riverine organic matter when mixed with seawater: Methodology and ecological implications

A dissertation
submitted in partial satisfaction of the requirements for the degree
Doctor in Science

By:

José Ernesto Sampedro Avila

Ensenada, Baja California, México
2024

A Dissertation Presented by

José Ernesto Sampedro Avila

And approved by the following Committee

Dr. Helmut Maske Rubach
Director de tesis

Dr. Juan Carlos Herguera García

Dra. María Asunción Lago Lestón

Dr. Zhanfei Liu

Dr. Rafael Andrés Cabral Tena
Coordinador del Posgrado en Ecología Marina

Dra. Ana Denise Re Araujo
Directora de Estudios de Posgrado

Resumen de la tesis que presenta **José Ernesto Sampedro Avila** como requisito parcial para la obtención del grado de Doctor en Ciencias en Ciencias en Ecología Marina

Floculación de materia orgánica de ríos cuando se mezcla con agua de mar: Metodología e implicaciones ecológicas

Resumen aprobado por:

Dr. Helmut Maske Rubach
Director de tesis

Como resultado de los aportes de nutrientes de los continentes a los estuarios y aguas costeras, florecimientos de fitoplancton son causas bien conocidas de agotamiento de oxígeno (<2 mg L^{-1}) en el fondo de estos ambientes acuáticos (hipoxia o "zonas muertas"). Además, la materia orgánica particulada (POM) también se forma abióticamente en la mezcla estuarina por floculación y/o adsorción de materia orgánica disuelta (DOM) de ríos, inducida por el incremento de cationes. Se ha observado floculación en estuarios y en simulaciones de laboratorio al mezclar agua de río con agua de mar, pero otros trabajos han encontrado un comportamiento conservativo de la materia orgánica. Estas inconsistencias posiblemente se expliquen por la composición química de DOM de los ríos, y sean controladas por variables ambientales (ej. concentración de cationes). La actividad microbiológica podría acelerarse como biopelícula en las partículas floculadas y así contribuir en agotar las concentraciones de oxígeno disuelto en estuarios y aguas costeras. El POM que se hunde podría incrementar la concentración de sustrato disponible para la respiración aeróbica en los ecosistemas bentónicos y así contribuir a la formación de "zonas muertas". El propósito de este trabajo fue documentar procesos que afectan el comportamiento de mezcla de materia orgánica (y métodos para estudiarla) y evaluar su relación con procesos ecológicos y su contribución a los ciclos biogeoquímicos. Se realizaron experimentos de laboratorio mezclando agua de mar con agua dulce de diferentes sitios (Baja California, California, Texas y Luisiana). Para la mayoría de los experimentos, los "end members" fueron prefiltrados antes de mezclarlos en diferentes proporciones. El agua mezclada y los miembros terminales de los experimentos se filtraron y fueron todos analizados para partículas orgánicas de carbono y nitrógeno (POC y PON). Las muestras de Texas se analizaron además para isótopos estables (δ^{13}C-POC y δ^{15}N-PON) y aminoácidos hidrolizables totales (THAA). Los filtratos de estas muestras también se analizaron para carbono y nitrógeno orgánicos disueltos (DOC y DON), nitrógeno inorgánico disuelto (DIN) y aminoácidos hidrolizables disueltos (DHAA). La mayoría de las muestras mostraron un comportamiento conservativo y sólo algunos experimentos dieron como resultado la floculación de DOM para formar POM. La ocurrencia de floculación se correlacionó con una mayor precipitación en las cuencas de drenaje de los cuerpos de agua (ríos, arroyos y presas). En algunos casos este patrón se atribuyó al transporte de materia orgánica terrestre, y en otros experimentos a una menor concentración de cationes divalentes en el agua dulce. Imágenes satelitales en aguas costeras del sur del Golfo de México (sGoM) indicaron una mayor entrada de sólidos totales suspendidos de los estuarios, y un aumento de la fluorescencia del fitoplancton por percepción remota al final de la temporada de lluvias. El incremento en el exporte de sólidos suspendidos podría estar relacionado con la floculación de materia orgánica o con la producción local de biomasa fitoplanctónica. La formación de POM por cualquiera de estos procesos podría causar las condiciones hipóxicas observadas en otros trabajos en la Laguna de Términos y cerca de la la desembocadura Grijalva-Usumacinta.

Palabras clave: Mezcla de agua de río con el océano, composición de la materia orgánica particulada y disuelta; transición de fase de materia orgánica disuelta a particulada

Abstract of the thesis presented **by José Ernesto Sampedro Avila** as a partial requirement to obtain the Doctor of Science degree in Marine Ecology

Flocculation of riverine organic matter when mixed with seawater: Methodology and ecological implications

Abstract approved by:

Dr. Helmut Maske Rubach
Thesis Director

As a result of nutrient inputs from continents to estuaries and coastal oceans, more frequent and intense phytoplankton blooms in these systems are well-known causes for oxygen depletion (<2 mg L^{-1}) in the bottom of these aquatic environments (hypoxia or "dead zones"). Moreover, particulate organic matter (POM) is also formed abiotically in estuarine mixing by flocculation and/or sorption of riverine dissolved organic matter (DOM), induced by the increase in cations. Flocculation has been observed in estuaries and laboratory simulations when mixing river water with seawater, but other works have found a conservative behavior of the organic matter. These inconsistencies are possibly explained by the chemical composition of riverine DOM, and the control by environmental variables (e.g. cations concentration). Microbiological activity could be accelerated as biofilm in the flocculated particles and thus contribute in the depletion of dissolved oxygen concentrations in estuaries and coastal waters. The sinking POM could increase the substrate concentration available for aerobic respiration in benthic ecosystems and thus contribute to the formation of "dead zones". The purpose of this work was to document conditions that affect the mixing behavior of organic matter (and methods to study it) and evaluate their relation with ecological processes and their contribution to biogeochemical cycles. Laboratory experiments were conducted by mixing seawater with freshwater from different sites (Baja California, California, Texas, and Louisiana). For most experiments, the end members were prefiltered before being mixed in different ratios. Mixed water and end members from experiments were later filtered and were all analyzed for particulate organic carbon and nitrogen (POC and PON). Samples from Texas were also analyzed for stable isotopes (δ^{13}C-POC and δ^{15}N-PON), and total hydrolyzable amino acids (THAA). Filtrates of these samples were also analyzed for dissolved organic carbon and nitrogen (DOC and DON), dissolved inorganic nitrogen (DIN) and dissolved hydrolyzable amino acids (DHAA). Most samples showed conservative behavior and only some experiments resulted in the flocculation of DOM to form POM. The occurrence of flocculation was correlated with higher rainfall in the drainage basins of the freshwater bodies (rivers, streams, and reservoirs). In some cases, this pattern was attributed to the transport of terrestrial organic matter, and in other experiments to a lower concentration of divalent cations in the freshwater. Satellite images in coastal waters of the southern Gulf of Mexico (sGoM) indicated a higher input of total suspended solids from estuaries, and an increase of remotely sensed phytoplankton fluorescence at the end of the rainy season. The increased export of suspended solids can bes related to flocculation of organic matter, or to local phytoplankton biomass production. POM formation from any of these processes might cause hypoxic conditions observed by other works in the Términos Lagoon and near the Grijalva-Usumacinta mouth.

Keywords: Mixing of river water with the ocean, composition of particulate and dissolved organic matter; the phase transition of dissolved organics to particulates

Dedication

To my eternal family.

Acknowledgements

I would like to thank the Centro de Investigación Científica y de Educación Superior de Ensenada, Baja California (CICESE) for the doctoral degree and for the student stipend received during the last months of my studies. CEMIEGEO (Centro Mexicano de Innovación en Energía Geotérmica) kindly enabled access to use the TOC analyzer for the experiments in Ensenada. CICESE administrative assistants and researchers always supported me in different ways.

The doctoral fellowship provided by the Consejo Nacional de Humanidades, Ciencias y Tecnologías (CONAHCYT) made it possible to study this doctorate. ConTex, a joint initiative of the University of Texas System and CONAHCYT, funded part of the research from my doctorate (Grant 2019-63A to committee members Dr. Maske and Dr. Liu). The University of Texas also partially funded my travels.

I am profoundly grateful to my committee members, Dr. Helmut Maske, Dr. Juan Carlos Herguera García, Dr. María Asunción Lago Lestón, and Dr. Zhanfei Liu, who dedicated their time to direct my project from the beginning of my doctoral studies.

The MicMar laboratory members, external collaborators, and other students always provided valuable feedback during meetings and informal talks. Some of them also helped during experiments and sample analyses: César Almeda, Esperanza Valdez, Paola Valdes, and Yessica Contreras.

Dr. Liu's laboratory members (University of Texas Marine Science Institute) also helped with comments and suggestions on experimental design and data interpretation. Dr. Kaijun Lu and Dr. Jianhong Xue's help with experiments and sample analyses made possible the research article that was published, including the preparation of the manuscript. Dr. Ryan Hladyniuk and M.Sc. Patricia Garlough from the UTMSI core facilities laboratory analyzed a great part of the samples from the experiments in Texas. Other UTMSI scholars, students, and administrative assistants always helped during my visits.

I am grateful to other students who coincided with me at CICESE during my doctoral studies, and supported me in different ways: Gabriela Reséndiz, Zurisaday Ramírez, Miguel Llapapasca, Diana Rodríguez, Fernando Alvarado, Omar Moreno, Yessica Loya, Angeles Orta, Arturo Fajardo, Laura, Kassandra Beltran, and others I might be forgetting.

I fulfilled this stage thanks to the support of my family and friends. Especially, I am very grateful to my wife Shalom and my son Helam, who always motivate me to do my best.

Table of contents

Page

List of figures

Figure Page

List of tables

Table Page

Chapter 1. General introduction

Estuaries are systems where freshwater from the river inflow is mixed with the seawater transported inward the continental basin by tide currents (Bianchi, 2007). Organic matter and other constituents from the river and seawater are mixed in these systems. Carbon-based compounds originated from organisms are generally referred as organic matter (OM). Generally, river water contains a higher load of organic carbon (up to 1,000 μM) than surface seawater (up to 150 μM) (Artemev, 1996). Worldwide rivers transport up to $400x10^{12}$ g C y^{-1} of organic carbon to coasts (Hansell & Carlson, 2015), and half of this carbon input is in the dissolved phase. Dissolved organic matter (<0.7 μm; DOM) can be transformed to particulate organic matter (>0.7 μm; POM), or inversely, along the salinity gradient in estuaries by means of dissolution, flocculation (Artemev, 1996), sorption (Hedges & Keil, 1999), photooxidation (Mayer et al., 2009), and biotic consumption and production (Wu et al., 2019). Organic matter which is not modified between these phases is considered to have a conservative mixing behavior. Biotic and abiotic processes in the estuarine mixing might also modify the chemical composition of organic matter.

A fraction of the DOM may aggregate by weak physical interactions after its electrostatic repulsion is neutralized by cations (Ca^{2+}, Mg^{2+}, Na^{+}) once being mixed in seawater (Gregory & O'Melia, 1989), considering the mainly negatively charged nature of natural organic matter. In addition, clay minerals in riverine waters can flocculate rapidly when exposed to the increased ions in estuaries (Kranck, 1984; Manning et al., 2011; Spencer et al., 2021), thus the subsequent sorption of DOM onto these aggregates can also lead to the formation of POM. Sorption of DOM to mineral particles has been extensively studied in turbid rivers in the field (Hedges & Keil, 1999), but this process has rarely been studied in low-baseflow small rivers. In estuarine waters, flocculation happens not only to DOM but also dissolved trace metals (Chenar et al., 2013; Karbassi et al., 2014; Karbassi & Heidari, 2015; Mayer, 1982; Millward & Liu, 2003; Tang et al., 2002; Valikhani Samani et al., 2015), mineral particles (Droppo et al., 1998; Hoyle et al., 1984; Moore et al., 1979; Zajączkowski, 2008) and nutrients (Asmala et al., 2022; Forsgren et al., 1996), although much less work has been done on DOM flocculation.

Organic matter transformation between particulate and dissolved phases is expected to be relevant for its remineralization potential in the coastal margins, since bacteria communities may preferentially consume a certain phase of organic matter (Amon & Benner, 1994; Gason & Kirchman, 2018; Jessen et al., 2017; Sivadon et al., 2019; Verdugo, 2012; Woebken et al., 2007). Besides the phase of organic matter,

composition is another important factor defining the possible remineralization potential (Biddanda & Benner, 1997; Findlay & Sinsabaugh, 2003; Thurman, 1985; Wangersky, 1984). For example, high molecular weight carbohydrates and total hydrolyzable amino acids are some main components of bulk DOM, and both of them are relatively labile (Harvey & Mannino, 2001). The composition of OM may also affect flocculation in turn, as OM sourced from higher plants, such as lignin-like components, tends to flocculate more due to its higher aromatic components and thus higher hydrophobicity (Mannino & Harvey, 2000; Meyers-Schulte & Hedges, 1986).

Rivers also transport high nutrients concentrations, that cause POM formation from phytoplankton biomass (Middelburg, 2019). Phytoplankton blooms frequency, intensity and extension have been reported to increase in the last decades (Anderson, 2007; Hallegraeff, 1993), and hypoxic or "dead" zones occurrence were suggested to increase due to this organic biomass that is used for aerobic respiration after sinking to the sediments (Diaz & Rosenberg, 2008; Rabalais et al., 2010). Flocculation of organic matter has not been considered to contribute oxygen depletion in coastal waters. This process is also relevant to better understand biogeochemical cycles.

1.1 Related work

Flocculation of up to 11% of the dissolved organic matter (humic substances and together with metals and phosphorus) from different rivers (Glen Burn, Luce, Stinchar and Cree) was observed shortly after mixing with seawater in the laboratory at salinities up to 20 (E. R. Sholkovitz, 1976). The addition of NaCl, $MgCl_2$ and $CaCl_2$ to flocculate the maximum amount of humic substances (up to 750 μg L^{-1}) in water from the Scottish river were determined as 0.1, 0.3, and 0.6 M, respectively (Eckert & Sholkovitz, 1976). High molecular weight dissolved humic substances were flocculated in a 1-hour laboratory experiment, but not observed in the dissolved organic carbon since the humic substances only represented 5% of the bulk dissolved organic matter (E. R. Sholkovitz et al., 1978). However, conservative behavior of dissolved organic matter (uncoupled with flocculation of iron) was observed in the Beaulieu (Moore et al., 1979) and the Severn (Mantoura & Woodward, 1983) estuaries, and in the Delaware Bay (Fox, 1983). Since the 1970 decade, flocculation has been documented sometimes in estuarine mixing (Asmala et al., 2014; Eckert & Sholkovitz, 1976; Forsgren et al., 1996; Fox, 1983; Furukawa et al., 2014; Ming & Gao, 2022; E. R. Sholkovitz, 1976; E. R. Sholkovitz et al., 1978), but conservative behaviors has also resulted in some studies (Ertel et al., 1986; Forsgren et al., 1996; Li et al., 2018; Mantoura & Woodward, 1983; Markager et al.,

2011; Moo valikhani 2015 re et al., 1979; Søndergaard et al., 2003). Other works have focused in studying the flocculation of metals (Chenar et al., 2013; Karbassi et al., 2014; Karbassi & Heidari, 2015; Mayer, 1982; Millward & Liu, 2003; Tang et al., 2002; Valikhani Samani et al., 2015) , minerals (Droppo et al., 1998; Hoyle et al., 1984; Moore et al., 1979; Zajączkowski, 2008) and nutrients (Asmala et al., 2022; Forsgren et al., 1996), but conditions that control the mixing behavior of organic matter are still unclear.

Laboratory and field studies conducted with water from the same rivers (Fox, 1983; E. R. Sholkovitz et al., 1978) indicated different mixing behaviors (flocculation and conservative behavior with the same river water) that suggested different involved processes. While only abiotic rapid aggregation or dissolution of organic matter might be relevant in short laboratory simulations, photochemical and biotic process affect dissolved and particulate organic matter amount and composition in the natural environment (Hernes & Benner, 2003; Mayer et al., 2009; Orellana & Verdugo, 2003; Wu et al., 2019). Thus, controlled experimental approaches were used in the present work to study the flocculation of riverine organic matter after being mixed with seawater.

Different methods have been used in the literature to observe flocculated organic matter in laboratory experiments and in the field, like total or particulate organic carbon analyses (E. R. Sholkovitz, 1976), humic substances analysis (Fox, 1983), and fluorescent dissolved organic matter measurement (Asmala et al., 2014). Some approaches have been considered in the present work to study flocculation of riverine organic matter after being mixed with seawater.

Microgels are self-assembly particles that occur spontaneously due to Ca^{2+} links (Verdugo, 2012), and are observed with fluorescence chlortetracycline labeling (Baltar et al., 2016; Ding et al., 2007). Alcian Blue (C. Xu et al., 2019) and Coomassie (Cisternas-Novoa et al., 2014) chemical reagents have been also used to quantify gel-like particles as transparent exopolymer particles (TEPs) and Coomassie staining particles (CSP).

The importance of the occurrence of flocculation to coastal environments has not been evaluated. Microbial communities may preferentially consume particulate or dissolved organic matter (Amon & Benner, 1994; Gason & Kirchman, 2018; Sivadon et al., 2019; Verdugo, 2012; Woebken et al., 2007) and thus implicate different remineralization and oxygen consumption in coasts (Jessen et al., 2017). Composition is another relevant factor for the preferential remineralization of the organic matter (Biddanda & Benner, 1997; Findlay & Sinsabaugh, 2003; Thurman, 1985; Wangersky, 1984) and therefore should be studied.

1.2 Justification

Determine the amount and conditions to flocculate dissolved organic matter in estuarine mixing is relevant for a better understanding of the carbon cycle and its effect on the oxygen consumption by microbial aerobic respiration in coastal environments.

1.3 Objectives

1.3.1 Main objective

Examine the mixing behavior of dissolved organic matter during estuarine mixing and its importance to coastal environments and contribute to the methodological approach to study this process.

1.3.2 Specific objectives

Quantify the flocculation of riverine organic matter in prefiltered and natural water from different sources.
Estimate the composition of the flocculated organic matter in laboratory experiments.
Investigate the potential artifact problems with the quantification of flocculation of dissolved organic matter.

Chapter 2. The chemical characteristics and mixing behaviors of particulate organic matter from small subtropical rivers in coastal Gulf of Mexico (Sampedro-Avila et al. 2024; *ECSS*).

2.1 Introduction

Rivers carry terrestrial organic matter along their drainage basins and discharge it into the ocean, contributing 400 × 10^{12} g C y^{-1} to the global ocean (Hansell & Carlson, 2015; Schlesinger & Melack, 1981). Commonly, riverine dissolved and particulate organic carbon (DOC and POC) concentrations (about 150-2500 µM and 100-1000 µM, respectively) are often higher than those in seawater (100–150 µM and 1–100 µM, respectively) (Artemev, 1996; Cao et al., 2018; Hedges, 1992), and more than 50% of the riverine organic matter is often in dissolved form (Hansell & Carlson, 2015; Meybeck, 1982). Organic matter (OM) is defined by size as either particulate (>0.7 µm; POM) or dissolved (<0.7 µm; DOM including colloidal form), but it is often transformed from one to the other phase through dissolution or flocculation along estuarine salinity gradients (Artemev, 1996). Organic matter transformation between particulate and dissolved phases is expected to be relevant for its remineralization potential in the coastal margins, since bacteria communities may preferentially consume a certain phase of organic matter (Amon & Benner, 1994; Gason & Kirchman, 2018; Jessen et al., 2017; Sivadon et al., 2019; Verdugo, 2012; Woebken et al., 2007). Besides the phase of organic matter, composition is another important factor defining the possible remineralization potential (Biddanda & Benner, 1997; Findlay & Sinsabaugh, 2003; Thurman, 1985; Wangersky, 1984). For example, high molecular weight carbohydrates and total hydrolyzable amino acids are some main components of bulk DOM, and both of them are relatively labile (Harvey & Mannino, 2001). The composition of OM may also affect flocculation in turn, as OM sourced from higher plants, such as lignin-like components, tends to flocculate more due to its higher aromatic components and thus higher hydrophobicity (Mannino & Harvey, 2000; Meyers-Schulte & Hedges, 1986).

The transformation of DOM to POM through flocculation has drawn attentions in recent decades. For instance, the flocculation of DOM has been considered an important mechanism of POM formation in estuaries (Asmala et al., 2014; Eckert & Sholkovitz, 1976; Forsgren et al., 1996; Fox, 1983; Furukawa et al., 2014; Ming & Gao, 2022; E. Sholkovitz et al., 1978; E. R. Sholkovitz, 1976; Wang & Gao, 2022). On the other hand, it has also been reported that riverine POM behaved conservatively after mixing with seawater (Ertel

et al., 1986; Forsgren et al., 1996; Y. Li et al., 2018; Mantoura & Woodward, 1983; Markager et al., 2011; Moore et al., 1979; Søndergaard et al., 2003). The term "flocculation" is used in different disciplines and with different meanings, but here it refers to the process that dissolved and colloidal components aggregate to form particles larger than the pore size of the kind of filter (0.7 μm) used to collect the particulates. Conservative behavior manifests itself when a compound within a dilution gradient shows concentrations that are proportional to the concentration difference between the two end members. It is assumed that a conservative compound does not change its phase state or chemistry during the dilution, which is often shown graphically by a linear concentration gradient between the two end members. Conservative behavior of POM or DOM has been reported in the downstream section of estuaries (Harvey & Mannino, 2001), where the salinity gradient often does not include the low salinity (1–15) region where flocculation is likely to occur (Asmala et al., 2014; Eckert & Sholkovitz, 1976; E. R. Sholkovitz, 1976). Moreover, for those studies that documented the non-conservative behavior of DOM, only a minor fraction of the bulk DOM (10%) was found to flocculate (Fox, 1983; Markager et al., 2011; E. R. Sholkovitz, 1976), making the detection of DOM flocculation more difficult.

A fraction of the DOM may aggregate by weak physical interactions after its electrostatic repulsion is neutralized by cations (Ca^{2+}, Mg^{2+}, Na^{+}) once being mixed in seawater (Gregory & O'Melia, 1989), considering the mainly negatively charged nature of natural organic matter. In addition, clay minerals in riverine waters can flocculate rapidly when exposed to the increased ions in estuaries (Kranck, 1984; Manning et al., 2011; Spencer et al., 2021), thus the subsequent sorption of DOM onto these aggregates can also lead to the formation of POM. Sorption of DOM to mineral particles has been extensively studied in turbid rivers in the field (Hedges & Keil, 1999), but this process has rarely been studied in low-baseflow small rivers. In estuarine waters, flocculation happens not only to DOM but also dissolved trace metals (Chenar et al., 2013; Karbassi et al., 2014; Karbassi & Heidari, 2015; Mayer, 1982; Millward & Liu, 2003; Tang et al., 2002; Valikhani Samani et al., 2015), mineral particles (Droppo et al., 1998; Hoyle et al., 1984; Moore et al., 1979; Zajączkowski, 2008) and nutrients (Asmala et al., 2022; Forsgren et al., 1996), although much less work has been done on DOM flocculation.

One way to evaluate the flocculation of OM is through measuring its optical properties, which are expected to change when organic matter or humic substances flocculate during the mixing of river water with seawater (Asmala et al., 2014). Through this technique, humic substances were found to aggregate in estuaries (Eckert & Sholkovitz, 1976; Ertel et al., 1986). Stable carbon isotopes and amino acid compositions indicate that the composition of organic matter can vary greatly along the salinity gradient

in estuaries (X. Li et al., 2018; Ming & Gao, 2022), but the observed variations could not be exclusively linked to flocculation because numerous other processes happen in an estuary, such as *in situ* production and degradation, strong resuspension and photooxidation. With very limited research investigating the estuarine mixing behavior of organic matter experimentally (Asmala et al., 2022; Forsgren et al., 1996; Fox, 1983; Furukawa et al., 2014; Mayer, 1982; Søndergaard et al., 2003; Valikhani Samani et al., 2015), laboratory simulation may be necessary to tease out the flocculation potential of DOM when river water mixes with seawater in estuaries.

Topography, soil composition, land use, and stream flow are relevant factors to determine the organic matter composition and concentration entering the estuaries and oceans (Hansell & Carlson, 2015). Generally higher streamflow rivers introduce a higher flux of organic carbon to coastal waters (Schlünz & Schneider, 2000), but some small coastal rivers with low base flow have higher carbon yields normalized to drainage basin area, compared with major rivers with higher overall carbon flux (Cai et al., 2016), thus being important for the regional coastal carbon budget. Mission and Aransas rivers of south Texas are two typical small rivers in northwestern Gulf of Mexico, with their watersheds next to each other but drastically different in terms of human influence.

The Mission River is more pristine and influenced by small shrubs, while the Aransas River drainage basin is dominated by agricultural fields and sewage treatment discharges (Mooney & McClelland, 2012; Reyna et al., 2017; Wu et al., 2019). As a result, the organic matter in the Mission River is mainly of terrigenous origin, while in the Aransas River organics originated mostly from agricultural crops and autochthonous phytoplankton (Lebreton et al., 2016; Lu & Liu, 2019; Wei et al., 2023; Wu et al., 2019; X. Xu et al., 2021).

The composition of DOM and POM is expected to differ between these two rivers depending on the flow conditions, yet this has not been addressed in a systematic manner. Conducting experiments with these two rivers, together with other rivers along the northwestern Gulf of Mexico, therefore, may allow us to understand the effects of organic matter composition on its mixing behavior.

The objectives here were to evaluate: (1) the water chemistry difference between Mission and Aransas rivers, including organic matter composition, and (2) the response of riverine POM when mixed with seawater under controlled laboratory conditions and how the mixing behavior may be affected by the composition of organic matter.

2.2 Materials and methods

2.2.1 Sampling sites, water collection and hydrographic measurements

Mission and Aransas are two typical small rivers in northwestern Gulf of Mexico. Water from these rivers drains in a South Texas estuary (Mission-Aransas Estuary), separated by approximately 23.5 km at the sampled locations (Fig. 1). Salinity and water hardness were similar in the two rivers (Table 1). Grasslands, shrublands, wetlands, and cultivated lands contribute approximately 3, 8, 10, and 17%, respectively, of the 400×10^{12} g C y^{-1} of total organic carbon exported from the continents to the ocean globally (Hansell & Carlson, 2015; Schlesinger & Melack, 1981). These land uses were represented on the drainage basins of the river water used for this work.

Water samples from Mission and Aransas rivers were manually collected in two years, December 2021 (both rivers), and September (Mission River) or October (Aransas River) 2022, using acid cleaned 10–20 L high density polyethylene carboys at freshwater sites (salinity of 0.5–0.8; Table 1). The climatic conditions differed between 2021 and 2022, with higher river flow in 2021 (546.5 and 198.2 m^3 s^{-1}) than 2022 (14.7 and 12.5 m^3 s^{-1}) in both rivers (Mission and Aransas, respectively). Water was also collected from the Trinity River, the Neches River, and the Atchafalaya River in October 2022 for additional experiments (Fig. S1, supplementary material). These three rivers flow to the northern Gulf of Mexico along the coasts of Texas and Louisiana. Seawater was collected from the Port Aransas Ship Channel during flood tide to minimize the contribution of estuarine water (Fig. 1).

The Ship Channel seawater represents typical coastal open Gulf of Mexico water in terms of water quality, organic matter, and phytoplankton community (Douglas et al., 2023a, 2023b). The collected water was kept in a dry cooler in darkness until returned to the laboratory (approximately 3 h). Hydrographic conditions of all water sources were measured in the field with a YSI 650 MDS (Multiparameter Display System) probe. Salinity was presented as Practical Salinity Units. Water hardness was measured with EDTA titration for all experimental treatments according to method 2340 C from Standard Methods for the Examination of Water and Wastewater protocol (APHA et al., 2012).

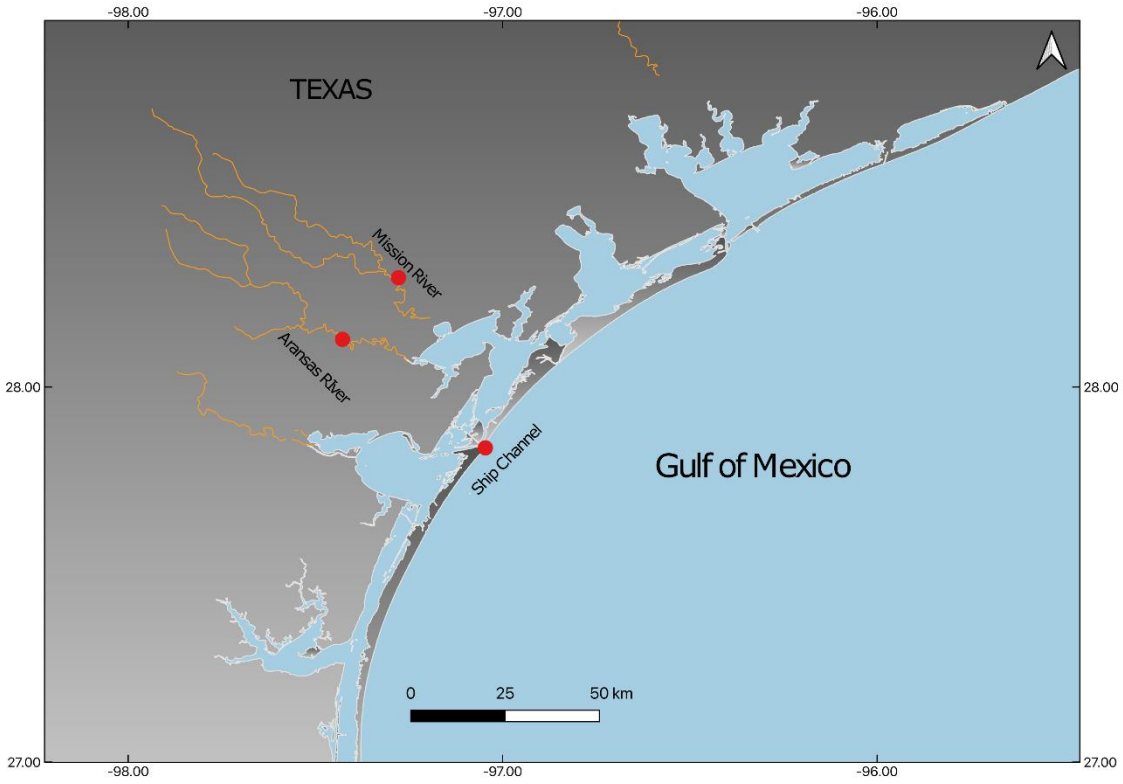

Figure 1. Location of sampling stations for the Mission River, the Aransas River, and the Port Aransas Ship Channel.

2.2.2 Mixing experiments

Water from each river was mixed with the seawater in different proportions yielding a total volume of 0.5 L (2021; duplicate bottles at each salinity) and 0.8 L (2022; triplicate bottles at each salinity) in polycarbonate squared bottles at a controlled temperature (20 ◦C). The series of mixed water included 0%, 20%, 50%, 80%, and 100% of freshwater from Mission and Aransas rivers in all experiments, and additional 70% and 90% in the 2022 experiments. Experiments with water from the Trinity, the Neches, and the Atchafalaya rivers only included 0%, 80%, and 100% freshwater in 2022. The bottles were gently stirred for 0.3 h on a shaker table (C2 Platform Shaker, New Brunswick Scientific) at 50 rpm and left to rest for 1 h in dark to avoid either breakup of aggregates or artificial promotion of flocculation (Burns et al., 2019; Guadayol et al., 2009; Mikkelsen et al., 2006). The < 2h time span was aimed to avoid any significant biological activities which might complicate the interpretation. The end members of 100% river water or seawater were treated the same as mixed water. About 100–700 mL samples from each bottle were filtered through 47 mm pre-combusted GF/F (Whatman) filters at controlled vacuum pressure (60 kPa). All filters were frozen (-20 ◦C) for later analyses of total hydrolyzable amino acids (THAA), POC, PON, δ^{13}C-POC, and δ^{15}N-PON. Filtered water for the end members was collected from the combusted filtration

Büchner flask and kept frozen (- 20 °C) until subsequent analyses of dissolved hydrolyzable amino acids (DHAA), dissolved organic carbon (DOC), total dissolved nitrogen (TDN), and dissolved inorganic nitrogen (DIN).

2.2.3 Elemental composition and stable isotopes analysis

The 47 mm GF/F filters with particles were punched with an 18 mm diameter hole cutter, and the punched filters were then dried at 60 °C for 18 h, later folded, and packed in tin capsules for analysis. Selected subsamples were exposed to HCl fumes for 24 h to remove the inorganic carbon before organic carbon analysis (Hedges & Stern, 1984). Non-acidified subsamples were used for PON and nitrogen isotope analyses (Lohse et al., 2000). A Thermo Fisher Scientific Flash EA-Isolink CNSOH elemental analyzer connected to a Thermo Fisher Scientific Delta V Plus isotope-ratio-mass-spectrometer was used to measure bulk POC, PON, and stable isotopes of POC (δ^{13}C-POC), and PON (δ^{15}N-PON). Isotopes results were presented using the conventional δ-notation (Equation 1):

$$\delta^{13}C\ (or\ \delta^{15}N) = \left[\left(\frac{R_{sample}}{R_{standard}}\right) - 1\right] (in\ ‰)$$

Where R_{sample} and $R_{standard}$ = $^{13}C/^{12}C$ (or $^{15}N/^{14}N$). δ13C-POC was expressed relative to the Vienna Pee Dee Belemnite (VPDB) scale and δ^{15}N-PON to the atmospheric signature (AIR) (Coplen, 1996). USGS-40 (δ^{13}C = - 26.39 ‰; δ^{15}N = - 4.52 ‰), USGS-41a (δ^{13}C = +37.63 ‰; δ^{15}N = + 47.57 ‰) reference standards and a casein internal standard solution were used for calibration. The internal standard casein was used to assess both the accuracy and precision of the analyses, yielding the precision for the C and N content was within 5%, and analytical error for δ^{13}C-POC and δ^{15}N-PON of 0.2% or lower.

2.2.4 Total (THAA) and dissolved hydrolyzable amino acids (DHAA) analyses

THAA and DHAA analyses were performed similarly except for the hydrolysis procedure. For THAA, 18 mm filter disks (punched from 47 mm GF/F, Whatman) were folded and inserted in combusted glass test tubes, and then 2 mL 6N HCl was added. For DHAA, 1 mL of filtered samples from the end members (water collected from the same combusted filtration Büchner flask used for filtering THAA with combusted GF/F) were transferred into pre-combusted glass test tubes and mixed with concentrated HCl to a final volume

of 2 mL and a final HCl concentration of 6N. All hydrolyzed samples were deoxygenated by gently sparging with ultrapure nitrogen gas (N_2) for 1 min, then vortexed, sparged again, and sealed tightly. All tubes were placed for hydrolysis in a Thermo Scientific Reacti-Therm III heating module for 20 h at 110 ◦C under N_2 (Kuznetsova & Lee, 2002). Two empty tubes with the adding of 2 mL 6N HCl only were treated the same as the samples for hydrolysis blanks.

After the hydrolyzed samples were cooled down, the liquid in each tube was filtered through glass wool to remove larger particles, and 0.5 mL of each sample were transferred to a combusted 6 mL vial and dried by sparging with N_2 (~30 min). Dried samples were resuspended in 0.5 mL water (LC/MS grade) and vortexed. An aliquot of 0.05 mL was then transferred to amber vials, with 0.55 mL LC/MS water and 0.4 mL methanol (LC/MS grade) added to each sample and vortexed for high performance liquid chromatography (HPLC) measurement. HPLC with fluorescence detection (Shimadzu) was used for THAA and DHAA analyses after pre-column *o*-phthaldialdehyde derivatization (C. Lee et al., 2000; Liu & Xue, 2020). Reference standards were used to quantify the following measured amino acids: aspartic acid/asparagine (ASP), glutamic acid/glutamine (GLU), histidine (HIS), serine (SER), arginine (ARG), glycine (GLY), threonine (THR), beta-alanine (BALA), alanine (ALA), tyrosine (TYR), gamma-aminobutyric acid (GABA), methionine (MET), valine (VAL), phenylalanine (PHE), isoleucine (ILE) and leucine (LEU). Relative standard deviations of replicate analyses varied generally within 10–20 %.

2.2.5 Dissolved organic carbon (DOC), total dissolved nitrogen (TDN), and dissolved inorganic nitrogen (DIN) analyses

A TOC-L analyzer (Shimadzu) was used for DOC and TDN analyses. Filtered water samples were transferred to 35 mL glass vials and automatically acidified by the instrument with 0.3 N H3PO4 and sparged for 1.5 min before 3 to 5 injections (200 µL) were measured. 1000 ppm C Organic Carbon Standard (CAT# SC021580–500C, SpectroPure) and 1000 ppm N Nitrate Nitrogen Standard (CAT# 5459-16, RICCA) were used for calibration. Low Carbon Water and Deep Seawater Reference from Hansell lab (University of Miami) were used to verify the calibration. Analytical errors of DOC analysis varied from 0.2 to 0.3%.

A QuickChem nutrient autoanalyzer (Lachat, 8500) was used to analyze inorganic nitrogen in 10 mL test tubes. Sulfanilamide and ammonium chloride were used throughout the sample runs to measure concentrations of ammonium and the sum of nitrates and nitrites. The total concentration of ammonium,

nitrates, and nitrites was subtracted from the TDN to calculate dissolved organic nitrogen (DON) for each sample.

2.2.6 Data analysis and statistics

All data analyses and plots were performed with the RStudio software (version 2023.03.1 + 446), using the package *tidyverse* (Wickham et al., 2019). An $\alpha = 0.05$ was considered for all statistical analyses. Data normality was evaluated with the Shapiro-Wilk's test and visually confirmed in a frequency histogram and a Q-Q plot. Bartlett's test was used to assess the homogeneity of variances. Outliers were identified with a Z score ($z > 3$). Welch's *t*-tests were used to compare measured values in one river with another in the same year and to compare the measured values in the same river but in different years. Statistical differences between the measured and the expected conservative values from the theoretical dilution line of the mixing diagrams were determined with paired *t*-tests.

The isotopic signature of the flocculated POC ($\delta^{13}POC_{floc}$) was calculated to examine whether the measured values significatively deviated from values calculated from conservative mixing (Equation 2):

$$\delta^{13}POC_{floc} = \frac{[POC_{meas}] \cdot [\delta^{13}POC_{meas}] - [POC_{cons}] \cdot [\delta^{13}POC_{cons}]}{POC_{floc}}$$

Where POC_{meas} was the measured POC [µM] in the experiments, $\delta 13POC_{meas}$ was the measured δ^{13}C-POC (‰), POC_{cons} was the predicted POC [µM] from conservative mixing at a given salinity, $\delta^{13}POC_{cons}$ was the predicted δ^{13}C-POC (‰), and POC_{floc} was the flocculated POC [µM] calculated from the difference between the measured and predicted values. THAA was calculated as the sum of the concentration of the sixteen measured amino acids. Carbon content in THAA (THAA-C) was calculated based on the number of carbon atoms in each amino acid. THAA-C contribution to bulk POC was also calculated (THAA-C/POC). A degradation index (DI) was calculated using the first two principal components of principal component analysis (PCA) based on the mole percentage (mole%) of each amino acid out of the THAA (Dauwe et al., 1999; Liu & Xue, 2020). The conservative mixing lines for POC, PON, and THAA of the experiments were calculated by connecting the data points of the riverine and the marine end members. POC/PON, δ^{13}C-POC, δ^{15}N-PON, and THAA-C/POC % were obtained as explained in the supplementary material (section "Calculation of mixing lines for POC/PON, POC-δ^{13}C, PON-δ^{15}N, and THAA-C/POC").

2.3 Results

2.3.1 The hydrological conditions and chemical characteristics of the river water

The height level maximum and the discharge values of Misson River were higher in the months before the 2021 experiments (in July 2021; 9.5 m and 546.5 m^3s^{-1}, respectively; Table 1) than before the 2022 experiments (in September 2022; 2.5 m and 14.7 m^3s^{-1}, respectively), according to the United States Geological Survey gage station (Refugio, TX – 08189500, https://waterdata.usgs.gov/monitoring-location/08189500/). A similar trend in water height level and discharge occurred for the Aransas River (Skidmore, TX – 08189700, https://wa terdata.usgs.gov/monitoring-location/08189700/), with higher values in 2021 (in September 2021; 9.9 m and 198.2 m^3s^{-1}, respectively) than in 2022 (in August 2022; 3.0 m and 12.5 m^3s^{-1}, respectively). These hydrological parameters defined flood conditions in 2021 and baseflow conditions in 2022, for both rivers.

In situ temperature in the river water used for the experiments varied from 20.1 to 25.5 °C, and dissolved oxygen (DO) from 5.5 to 10.8 mg L^{-1} (Table 1; Table S1, supplementary material) within the different rivers. Salinity, pH, and water hardness were similar within most of the different river water sources used for the experiments (Table 1; Table S1, supplementary material), except the Neches River with values of 3, 7.7, and 354 mg $CaCO_3$ L^{-1}, respectively. Specifically, water hardness was similar in the Mission River (125–163 mg $CaCO_3$ L^{-1}) and the Aransas River (119–131 mg CaCO3 L^{-1}) in both years (Table 1). The higher DIN value was measured in the Aransas River in 2021 (128 µM), but it was only 1.4 µM in 2022. DIN values in the Mission River were similar in both years (6–7 µM).

The POC and PON concentrations in all rivers were higher than those of the seawater from the Port Aransas Ship Channel (Table 1). Similar POC mean values were measured in the Mission River in 2021 (147 µM; Table 1), the Aransas River in 2022 (150 µM), and the Trinity River (111 µM; Fig. S2a; Table S1; supplementary material), which were higher than concentrations in other rivers (Fig. S2a, supplementary material). Based on sampling time, the POC concentration in the Mission River was significantly higher in 2021 (147 µM) than in 2022 (83 µM; Fig. 2a; $p = 0.047$). Based on sampling location, the POC concentration in the Mission River was not significantly different from that in the Aransas River in 2021 (Table 1; $p = 0.06$). The highest PON value was measured in the Aransas River in 2022 (22 µM; Table 1), significantly

higher than the same river in 2021 ($p < 0.001$), while the lowest PON value was measured in the Mission River in 2022 (8 µM; Table 1).

Table 1. Hydrographic conditions, sampling coordinates in the Mission and Aransas rivers, and the different parameters measured in the two years of the experiments.

	Sampled river (date)			
	Mission River (Dec/2021)	**Aransas River (Dec/2021)**	**Mission River (Sep/2022)**	**Aransas River (Oct/2022)**
Latitude	28.29	28.13	28.29	28.13
Longitude	-97.28	-97.43	-97.23	-97.43
Hardness (mg $CaCO_3L^{-1}$)	163	131	125	119
Salinity	0.71	0.55	0.78	0.58
pH	7.29	7.39	7.62	7.89
DO (mg L^{-1})	10.79	9.54	5.49	6.88
Drainage basin land use[a]	Pristine shrubs	Agriculture and sewage treatment	Pristine shrubs	Agriculture and sewage treatment
Flow conditions[b]	Flood	Flood	Baseflow	Baseflow
Gage height in annual peak (m)[b]	Jul/2021: 9.5	Jul/2021: 9.9	Sep/2022: 2.5	Aug/2022: 3.0
Streamflow in annual peak (m^3 s^{-1})[b]	Jul/2021: 546.5	Jul/2021: 198.2	Sep/2022: 14.7	Aug/2022: 12.5
Probable main DOM source[c]	Terrestrial	Terrestrial	Autochthonous phytoplanktonic	Autochthonous phytoplanktonic
POC [µM]	147	105	83	150
PON [µM]	14	13	8	22
POC/PON	10.1	7.9	9.7	6.9
δ^{13}C-POC (‰)	-28.4	-25.9	-29.4	-30.9
δ^{15}N-PON (‰)	4.6	7.1	16.8	9.6
PIC [µM]	29	7	15	7
THAA [µM]	4.0	1.8	3.4	7.1
THAA-C/POC (%)	11.5	7.3	17.5	20.7
DI	-5.4	-3.3	-2.4	1.3
DOC [µM]	340	518	617	459
DON [µM]	22	119	30	26
DOC/DON	15.5	4.4	20.3	17.8
DIN [µM]	6	128	7	1.4
TDAA [µM]	1.3	0.9	--	--

-- Not measured. [a]Mooney & McClelland, 2012; Reyna et al., 2017; Wu et al., 2019. [b]USGS gages 08189500 (Mission River) and 08189700 (Aransas River). [c]Lu & Liu, 2019.

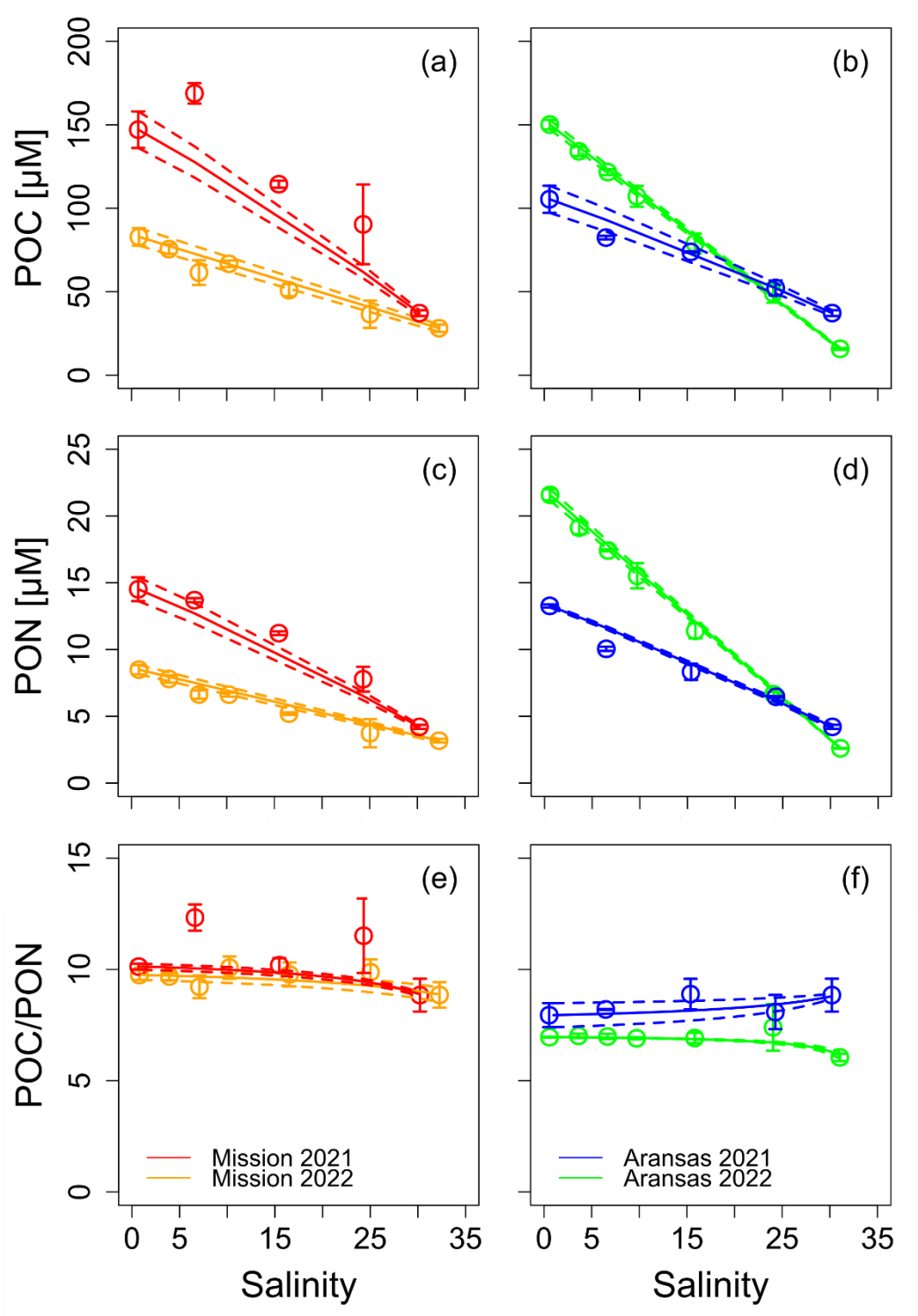

Figure 2. Bulk particulate organic carbon (POC; a-b), particulate organic nitrogen (PON; c-d) and POC/PON ratio (e-f) from laboratory experiments with river water mixed with seawater at different proportions. Mean values from experimental treatments with (a, c, e) Mission River water represented with red (2021) and orange (2022) circles, and (b, d, f) Aransas River water in blue (2021) and green (2022). The conservative mixing lines calculated from end member concentrations are shown as solid lines. Error bars and dotted lines represent the standard deviation (n=2 in 2021 and n=3 in 2022 experiments).

The PON value in the Mission River end member (14 μM) was not significantly different from the Aransas River in 2021 (13 μM; p = 0.29), but significantly higher than the Mission River in 2022 (8 μM; p = 0.046). POC/PON ratios in the Mission River end member from both 2021 (10.1; Table 1) and 2022 (9.7) experiments were higher than other rivers (Table 1; Fig. S2c, supplementary material).

The lowest POC/PON ratio was measured in the Trinity River end member (5.3; Fig. S2c; Table S1; supplementary material). POC/PON in the Port Aransas Ship Channel seawater was similar within the experiments (Fig. 2e–f), except in the experiment with the Aransas River in 2022 (6.0). The most depleted δ^{13}C-POC values were observed in the Trinity River (- 32.3 ‰; Table S1; supplementary material), the Neches River (-30.9) and the Aransas River (- 30.9 ‰; Table 1) from 2022, while the most enriched value was from the Aransas River in 2021 (- 25.9 ‰), similar to the seawater in the same experiment (- 25.5 ‰). δ13C-POC was similar in the Mission River end member in both years (Table 1), The most enriched δ15N-PON value from all experiments was measured in the Mission River end member in 2022 (16.8 ‰; Table 1). The Mission River in 2021 had the most depleted δ^{15}N-PON mean value (4.6 ‰, Table 1), even lower than the seawater in that experiment (7.0 ‰). The seawater generally had a similar δ^{15}N-PON signature to the river water, except the Mission River water in 2022. The river water had higher total THAA concentrations than the seawater from most experiments (Fig. 3c–d). THAA in the Aransas River end member in 2022 was higher (7.1 μM, Table 1) than in the Aransas River in 2021 (1.8 μM; p = 0.004). THAA-C/POC in river water varied from 7.3% to 20.7% (Fig. 3e–f), similar to the seawater value from each respective experiment. Individual amino acids mole percentages from the river water and the seawater were generally similar in all the experiments. GLY (18%, based on all end members) was the most abundant one, followed by ALA (13%); while GABA (0.2%) and MET (<0.001%) had the lowest abundance of all amino acids. Calculated degradation index (DI) values for different end members ranged from - 5.4 to 4.9, and there were no significant differences observed in DI between most experiments, except when comparing the Mission and Aransas end members from 2022 (Table 1; p = 0.003).

2.3.2 The mixing behavior of riverine POM after being mixed with seawater

Significantly different results ($p < 0.05$; Welch's *t*-tests and paired *t*-tests) from predicted values by the mixing line are considered non-conservative. If no gains or losses were observed in POM, the measured amount must result in the corresponding proportions of the two endmembers (river water and seawater) according to physical mixing. POC behaved conservatively in six out of seven mixing experiments conducted in this work (Fig. 2a–b; Fig. S2, supplementary material). However, in the experiment conducted

in 2021 with Mission River water, the POC values measured were significantly higher than the predicted conservative value when comparing all mixing proportions together with the paired *t*-test ($p = 0.003$; Fig. 2a). The most significant POC addition was found at salinity of 6 (corresponding to 20% seawater + 80% river water), with an increase of 41 µM (32%) over the predicted value ($p = 0.036$). Consistently, PON also behaved conservatively in most experiments except in the Mission River in 2021 with a mean difference of 1 µM ($p = 0.003$).

The molar C/N ratios of particles, or POC/PN, were conservative in most mixing experiments, except for Mission River in 2021 at the salinity of 6 (12.3), which was higher than the conservative mixing value (9.9; Fig. 2e). This difference of the mean POC/PON to the mixing value was consistent with the flocculated POC in that experiment (Fig. 2a).

δ^{13}C-POC was also non-conservative in the Mission River mixing experiment in 2021 (29.7 ‰; Fig. 3a), coinciding with the POC aggregation in the experiment (Fig. 2a). A conservative mixing behavior of δ^{15}N-PON was observed in all experiments (Fig. S3, supplementary material), even when PON flocculation was observed in Mission River from 2021 (Fig. 2c). The original mixing curve of the Mission River experiment in 2022 was optimized with a $^{15}N/^{14}N$ ratio (0.003729911) in the riverine end member, to obtain the best fit to the measured data averages ($R^2 = 0.85$).

The Aransas River experiment from 2021 resulted in additional THAA from the expected conservative mixing behavior ($p = 0.014$; Fig. 3d), even when bulk POM was conservative. THAA addition was also apparent in the Mission River in 2021 at a salinity of 6, but not significant ($p = 0.15$). THAA behaved conservatively after mixing the river water with seawater in all other experiments (Fig. 3c–d). In the Mission River experiment from 2021, the THAA-C/POC mean value was below the mixing line at all mixing proportions (Fig. 3e), whereas THAA-C/POC in the Aransas River from 2021 was above the mixing line. This parameter was conservative in all other experiments (Fig. 3e–f).

δ^{13}C-POC was non-conservative in the Mission River mixing experiment in 2021 (-29.7 ‰; Fig. 3a), coinciding with the POC aggregation in the experiment (Fig. 2a). A conservative mixing behavior of δ^{15}N-PON was observed in all experiments (Fig. S3, supplementary material), even when PON flocculation was observed in Mission River from 2021 (Fig. 2c). The original mixing curve of the Mission River experiment in 2022 was optimized with a ^{15}N abundance (0.03158) in the riverine end member, to obtain the best fit to the measured data averages ($R^2 = 0.85$).

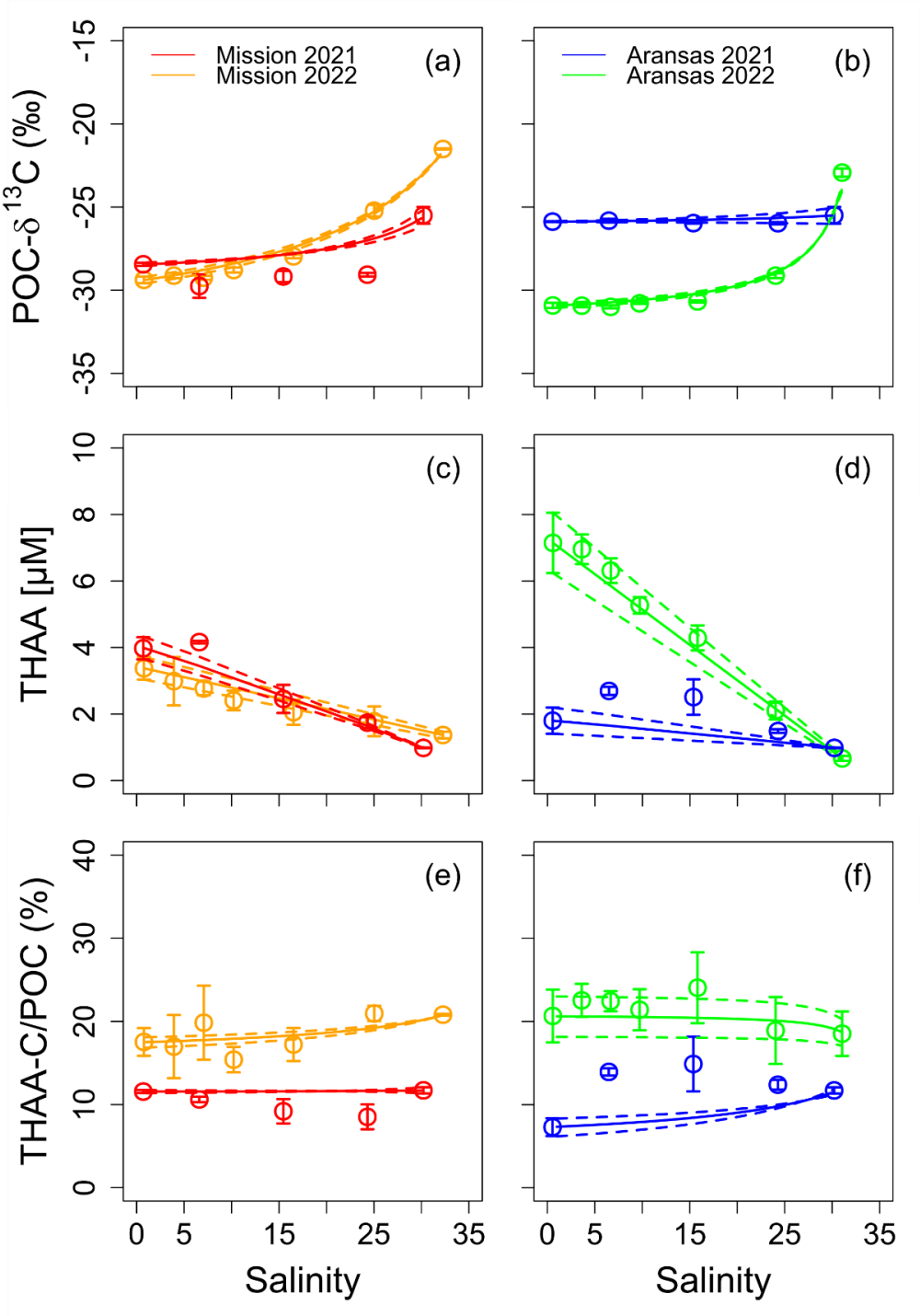

Figure 3. Bulk particulate organic δ13C values (POC-δ13C; a-b), total hydrolyzable amino acids (THAA; c-d), THAA carbon contribution to bulk POC (C-THAA/POC; k-l), from laboratory experiments with Mission River and Aransas River (Texas) water, both mixed with seawater at different proportions. Mean values from experimental treatments with Mission River water are represented with red (2021) and orange (2022) circles, and data from Aransas River water are in blue (2021) and green (2022). Conservative mixing lines calculated from end members are solid. Dotted lines and error bars represent the standard deviation (n=2 in 2021 and n=3 in 2022 experiments).

The Aransas River experiment from 2021 resulted in additional THAA from the expected conservative mixing behavior ($p = 0.014$; Fig. 3d), even when bulk POM was conservative. THAA addition was also apparent in the Mission River in 2021 at a salinity of 6, but not significant ($p = 0.15$). THAA behaved conservatively after mixing the river water with seawater in all other experiments (Figs. 3c-d). In the Mission River experiment from 2021, the THAA-C/POC mean value was below the mixing line at all mixing proportions (Fig. 3e), whereas THAA-C/POC in the Aransas River from 2021 was above the mixing line. This parameter was conservative in all other experiments (Figs. 3e-f).

2.4 Discussion

2.4.1 The different chemical characteristics of POM between Aransas and Mission rivers

Bedrock composition determines ion abundances (e.g. Ca and Mg) in continental surface freshwater (Rosborg et al., 2015). The water hardness in the Mission and Aransas rivers was similar due to the physical proximity between the two drainage basins. For example, the sampling stations at the two rivers are separated by only 23.5 km. However, organic matter and inorganic nitrogen values varied greatly within the rivers because of different land uses and human influence in the two drainage basins (Mooney & McClelland, 2012; Reyna et al., 2017; Wu et al., 2019).

The remarkably high DIN value in the Aransas River in 2021 (128 µM) indicated an input of nutrients by sewage treatment plants and/or agriculture fields in its drainage basin. The input of wastewater treatment plants can make up to 78% of the freshwater in Aransas River during baseflow conditions (Mooney & McClelland, 2012). A study has shown that up to 70% of dissolved nitrates supplied by the Aulne, Elorn, and Penfeld rivers to the Bay of Brest, France, can come from agricultural sources (Monbet et al., 1981). Consistently, Wu et al. (2019) also reported much higher DIN values in Aransas River (25 µM) than Mission River (3 µM) in samples collected in January 2016 at the same locations as the present work. However, the magnitude of the difference may depend on season and floods/droughts conditions. For example, the DIN concentration of Aransas River was only 1.4 µM in 2022, even less than that of Mission River (7 µM). This may reflect a much lower input of nutrients due to dry conditions in 2022. *In situ* production of phytoplankton may have also contributed to this low level of DIN in Aransas River, as evidenced by the

high THAA, POC, and PON concentrations and a C/N value (6.9) close to Redfield Ratio. Similarly, nitrate concentrations in the Swan and the Blackwood estuaries increased during the rainfall months, due to rivers input with drainage basins influenced by agricultural activities (Hodgkin & Lenanton, 1981). An increase of POC and PON (150 and 22 μM, respectively) coincident with a decrease of DIN (1.4 μM) in the Aransas River endmember from 2022 (Table 1) suggested phytoplankton growth (Han et al., 2022).

The Mission River is more pristine than the Aransas River, and its drainage basin is dominated by shrubs (Mooney & McClelland, 2012; Reyna et al., 2017; Wu et al., 2019), as clearly indicated by the lower DIN value (6–7 μM) in both 2021 and 2022. This nutrient level is consistent with previous studies (Wei et al., 2022; Wu et al., 2019). Terrestrial organic matter contribution in the Mission River was hinted by the higher POC/PON (10.1; Table 1), higher DOC/DON (15.5), and lower DI (- 5.4) than in the Aransas River in 2021. High-flow events have been documented to introduce more terrestrial organic matter from the drainage basin to the Mission River (Lebreton et al., 2016; Mooney & McClelland, 2012; Wei et al., 2022). Other relatively pristine rivers, the Yukon, the Collesville, Trinity, and the Pearl, are documented to export higher carbon yields (exported carbon normalized to drainage basin area) with a probable dominance of terrestrial material, than rivers more influenced by human activities, like the Mississippi (Cai et al., 2016). However, some rivers, like the Yukon River, have much higher discharge volumes (typically up to 18, 000 $m^3\ s^{-1}$) (Pilot Station, AK – 15565447, https://waterdata.usgs.gov/ monitoring-location/15565447/) than the Mission River (546.5 and 14.7 $m^3\ s^{-1}$ in 2021 and 2022, respectively) (Table 1). High river inflow must be needed then to carry the terrestrial organic matter to contribute mainly to the bulk POC in its water as with the Yukon River, which only happened in 2021 in the Mission River. Consistently, subtropical Pearl River exported more POC in the wet season (Spring) than in the dry season (Summer) (Cai et al., 2016).

Carbon stable isotopes or $\delta^{13}C$ have often been used to differentiate sources of organic matter in estuarine waters, as terrestrial C3 plants have depleted ^{13}C values (-25‰) while marine algal matter is more enriched (-18 to -22‰). However, the assignment may become complicated when there is a source from C4 plants such as Spartina (-13‰) (Fry, 2006; Peterson & Fry, 1987). Judged from the much depleted $\delta^{13}C$ values (-25.9 to - 30.9 ‰) in both Mission and Aransas rivers and both in 2021 and 2022, there should not be much contribution from C4 plants in the riverine organic matter, even though there are abundant C4 plants from agriculture activities in the Aransas River drainage basin (Mooney & McClelland, 2012; X. Xu et al., 2021). The results are also consistent with those of Wei et al. (2022), with an average $\delta^{13}C$-POC of -32‰ for both Aransas and Mission Rivers. While C3 plants contribution might be able to explain the very depleted $\delta^{13}C$-POC values (-25.9 to -30.9 ‰, Table 1) in both rivers, it could not explain the low C/N ratios (7.9–10.1) and

high concentrations of PON and THAA. Instead, we argue that *in situ* production may have contributed significantly to the POM and its depleted $\delta^{13}C$ values in the two rivers. Even during the high flow conditions in 2021, the flow rates were only in the range of 198–546 $m^3\ s^{-1}$, and these rates are still much lower than typical rivers (Nijssen et al., 2001; Van Vliet et al., 2013).

Low base flow conditions will result in less turbidity and thus facilitate algal growth. For example, the high contribution of phytoplankton biomass to POM in the Aransas river is clearly hinted by higher PON (22 µM; Table 1), THAA (7.1 µM), THAA-C/POC (20.7%), and high DI (1.3) value or freshness in 2022, to a lesser extent in 2021 and for Mission River in both 2021 and 2022. It is unclear yet why the phytoplankton in these two rivers has these relatively depleted $\delta^{13}C$-POC values values, but it may be related to the 13C value of dissolved inorganic carbon (DIC), the growth rate of algae, and the dominance of cyanobacteria in the lower streams of the two rivers (Chanton & Lewis, 1999; Pancost et al., 1997; Wei et al., 2023). Cyanobacteria, with high surface area to volume ratios, should have low fractionation during photosynthesis driven by higher carbon demand (Rau et al., 1996), but this has not been systematically examined in this region. Nevertheless, the possibility of high fractionation of cyanobacteria is consistent with the results of Reyna et al. (2017), where they showed that $\delta^{13}C$ values of POC were more depleted when cyanobacteria were the major algal species in the adjacent Mission Aransas Estuary. Isotope fractionation by specific algae taxa is complicated and driven by the physiology and geometry of the algae, together with the environmental factors, thus more work is needed to elucidate how the inorganic carbon is fractionated by cyanobacteria, dominated by Cyanobium in this region (Reyna et al., 2017), in the riverine environment of Aransas and Mission rivers.

Allochthonous POM from terrestrial sources including agricultural crops should also contribute to the Aransas River water, especially during flood conditions (Lebreton et al., 2016). More transport of organic matter from the continent potentially occurred during flood conditions in 2021 than in 2022 (Lu & Liu, 2019), as indicated by the significantly higher water level (9.5 and 9.9 m) and discharge rate (546.5 and 198.2 $m^3\ s^{-1}$) in 2021 for both rivers (Mission and Aransas, respectively). Although the data overall indicated the dominance of *in situ* production from both rivers and in both years, POM in Mission River seems to contain more allochthonous POC as evidenced by the higher C/N ratios (9.7–10.1) and lower DIs (- 24 to - 5.4) than those in Aransas River. This trend was more evident in 2021 than in 2022. The $\delta^{15}N$-PON results offered another angle to the biogeochemical processes of these two rivers. The $\delta^{15}N$-PON were much more enriched in Mission River in 2022 (16.8‰) than in 2021 (4.6‰). The $\delta^{15}N$-PON values in Aransas River were similar, but only slightly higher in 2022 (9.6‰) than 2021 (7.1‰), a trend similar to

Mission River. Consistently, Xu et al. (2021) reported that the $\delta^{15}N$ of organic matter in surface sediments (<1 cm) was in the range of 5.6–10.4‰ in the lower stream of the two rivers. The $\delta^{15}N$-PON in these rivers are collectively controlled by terrestrial plants and crops, sewage treatment discharge, algal production, and benthic denitrification. The observed values (4.6–16.8‰) are more enriched than typical terrestrial plants (~2.8‰) (Dawson et al., 2002), suggesting the role of sewage treatment discharge. However, the benthic denitrification can also strongly fractionate the nitrate considering the low baseflow of these rivers, or strong benthic-pelagic interactions. This process may explain the highly enriched $\delta^{15}N$-PON signal in the Mission River in 2022 (16.8‰), as extensive denitrification in the sediments may lead to highly enriched $\delta^{15}N$-nitrate in the water column which were subsequently assimilated by phytoplankton (Kritee et al., 2012).

2.4.2 POM in most small subtropical rivers is conservative in estuarine mixing except the Mission River in 2021

Bulk POM in most mixing experiments, including those with water from the Atchafalaya, Neches, and Trinity rivers (Fig. S2, supplementary material), behaved conservatively. Conservative POC/PON, $\delta^{13}C$-POC, $\delta^{15}N$-PON, THAA, and THAA-C/POC (Figs. 2–3; Figs. S1–S2, supplementary material) showed that neither the amount nor the composition of this organic matter changed after being mixed with seawater. In other words, organic matter did not undergo flocculation or dissolution during the mixing, which otherwise would affect the POM concentrations and mixing had been reported previously (Ertel et al., 1986; Forsgren et al., 1996; Y. Li et al., 2018; Mantoura & Woodward, 1983; Moore et al., 1979; Søndergaard et al., 2003). However, flocculation was found when the behavior of humic substances (Asmala et al., 2014; Benner & Opsahl, 2001; Eckert & Sholkovitz, 1976; E. Sholkovitz et al., 1978) and lignin phenols (Hernes and Benner, 2003) (Hernes & Benner, 2003) were studied. Other studies also observed the flocculation of riverine bulk organic matter (Asmala et al., 2014; Eckert & Sholkovitz, 1976; Forsgren et al., 1996; Fox, 1983; Furukawa et al., 2014; Ming & Gao, 2022; E. Sholkovitz et al., 1978; E. R. Sholkovitz, 1976). Therefore, the present work provides valuable information not only on the occurrence or not of this flocculation, but also on the composition of the resulting organic matter (i.e. $\delta^{13}C$-POC, $\delta^{15}N$-PON, THAA).

Particularly, flocculation was observed in the Mission River experiment from 2021 ($p = 0.002$ Fig. 2a), where the strongest signal of POM addition in the Mission River occurred at the mixing proportion of 20% of seawater and 80% of river water ($p = 0.036$, Fig. 2a). Seawater did not contribute much DOM to the

mixed water (18 µM of DOC and 1 µM of DON at salinity of 6), and the increase of salinity to a value of 6 was enough to form POM from the flocculation of DOM (Asmala et al., 2014; Søndergaard et al., 2003; Valikhani Samani et al., 2015). The formed POM amount (41 µM) also had a similar percentage (12%; 41 µM/340 µM, Table 1) with literature regarding the flocculation of approximately 10% of the DOM in the river water (Forsgren et al., 1996; Fox, 1983; E. R. Sholkovitz, 1976). Natural seawater ion concentrations are relatively constant worldwide (Millero, 2016), thus POM formation controlled by salinity might be expected at the same salinity values as the literature (Eckert & Sholkovitz, 1976; Harvey & Mannino, 2001; E. R. Sholkovitz, 1976). The reproducibility of these results was favored by using natural seawater, and issues of artificial seawater preparation observed in preliminary experiments of the present work, like organic matter contamination and precipitate formation, were avoided. Marine organic matter contribution should not be substantial, because marine DOC and POC after mixing 20% of seawater and 80% of river water (salinity of 6) contributed about 4% and 2%, respectively, of the resulting concentrations. Because of similar cation concentrations in the Mission and Aransas rivers (confirmed by salinity and water hardness; Table 1), differences in mixing behaviors observed between experiments should then be attributed to the differences in organic matter composition of these two rivers.

This flocculation of DOM may be related to the clay minerals, which also tend to flocculate at lower salinities in estuaries (Keil et al., 1997; Kranck, 1984; Spencer et al., 2021), if there is strong sorption of DOM to these clay minerals (Hedges & Keil, 1999). However, this possibility is low because the Mission River has a very low baseflow (Refugio, TX – 08189500, https://waterdata.usgs.gov/monitoring-location/08189500/) and thus should contain a low concentration of total suspended solids with respect to POM concentration. This could be observed with the particulate inorganic carbon (PIC) of 18–20% measured in non-acidified filters (Table 1), relative to the POC amount in the end members. Biotic and photochemical processes (Hernes & Benner, 2003; Orellana & Verdugo, 2003) can also be excluded with the experimental design used here, with a very short mixing regime (<2 h) and under dark conditions.

In addition to the higher POC concentrations, also observed were the enrichment in POC/PON and depletion in δ^{13}C-POC, respective to the mixing line (Figs. 2 and 3). These POC/PON and δ^{13}C-POC deviations from the mixing lines of each parameter indicated a different composition of the flocculated organic matter (41 µM) compared with the expected bulk POM. The higher C/N ratios (12.3), and more depleted δ^{13}C of the flocculants suggest that dissolved DOM sourced from terrestrial plants was preferentially flocculated. This is consistent with the fact that the amount of terrestrial organic matter in the Mission River may be higher in 2021 due to its high flow conditions (Table 1) (Baltar et al., 2016; Findlay

& Sinsabaugh, 2003). The lower $\delta^{13}C$ value of the flocculants may be indicative of terrestrial sources of lignins or lipids such as leaf waxes, which tend to be more depleted in $\delta^{13}C$ (Benner, 1991; S. A. Lee et al., 2020; Smith & Epstein, 1971). Although high flow conditions in 2021 may be able to explain the extra contribution of terrestrial DOM to Mission River, it is not entirely clear why the flocculation was not observed in the 2022 experiment, when the rivers carried even higher DOC concentration and C/N ratio. Further work on specific organic compounds, such as lignin and lipids, is needed to elucidate the mechanistic processes of the flocculation.

Overall, it appears that under most conditions the POM behaved conservatively in estuaries along the northern and western Gulf of Mexico, meaning that in a short time scale there is no flocculation of DOM or dissolution of POM in the estuaries. Although we were able to tease out the physical control on the organic matter transformations in estuaries in laboratory settings, under the field conditions processes such as photochemical reactions and biological degradation can be extremely dynamic, occurring in hours to days and thus affecting the formation and dissolution of POM (Mayer et al., 2009; Wu et al., 2019). In addition, we found significant flocculation in Mission River in 2021, which may be important in controlling the biogeochemical cycling of riverine organic matter should the right conditions that lead to flocculation exist in certain rivers and in certain seasons. Grasslands, shrublands, and wetlands contribute about 20% of the total organic carbon globally exported to the ocean (400×10^{12} g C y^{-1}) (Hansell & Carlson, 2015; Schlesinger & Melack, 1981). Given that half of the total organic carbon can be found as DOC (Hansell & Carlson, 2015; Meybeck, 1982), and a flocculation rate of 12% recorded in this work, it can be roughly estimated that on a global scale grasslands, shrublands, and wetlands might contribute up to 4.8×10^{12} g C y^{-1} of flocculated DOC to form POC, as an upper bound estimate.

2.5 Conclusions

Organic matter from two small subtropical rivers, Aransas and Mission, in the northwestern Gulf of Mexico was chemically characterized in a systematic manner. The results showed that while the Aransas River is more influenced by human activities, *in situ* production was the major contributor to the POM in both 2021 and 2022 with relatively low baseflow in both rivers. The mixing behavior of organic matter in estuaries depends on ecological and environmental factors, and to evaluate the flocculation controlled by physical processes, laboratory experiments were designed by mixing riverine water from Mission, Aransas, and other rivers with adjacent seawater in different proportions. The results showed that bulk POM,

together with the composition of POM, generally behaved conservatively during the mixing, suggesting that neither dissolution nor aggregation occurred. However, significant flocculation was observed in the Mission River from 2021, coincident with depleted δ^{13C}-POC and higher POC/PON than predicted, which suggested that DOC sourced from C3 plants was preferentially flocculated. While it is unclear exactly why the Mission River water flocculated, it is likely that 2021 was a relatively wet season that may have resulted in increased input of terrestrial organic matter from the drainage basin of the more pristine Mission River. Earlier literature had suggested that terrestrial organic matter abundance together with increased levels of humic substances might control the flocculation process. While more work is needed to elucidate the exact organic components that are likely to be flocculated, results from this work suggest that in tropical and subtropical rivers, which are often subject to episodic flood events, the flocculation of DOM during the mixing can be substantial under right conditions. The settlement of the flocculants may further trigger the degradation of organic matter, consumption of dissolved oxygen, nutrient regeneration, etc., in the subsurface water and surface sediment (Liu & Xue, 2020).

Chapter 3. Mixing behavior of organic matter in prefiltered freshwater from California and Baja California

3.1 Introduction

Flocculation of DOM and other dissolved components (e.g. iron and phosphate) in estuarine mixing is expected to occure with increasing cation concentration as the seawater salinity increases (Asmala et al., 2014; Eckert & Sholkovitz, 1976; E. Sholkovitz et al., 1978; E. R. Sholkovitz, 1976). Cations reduce electrostatic repulsion of organic molecules and enhance their aggregation to form POM (Gregory & O'Melia, 1989). Seawater calcium concentration is relatively constant worldwide and generally much higher than in freshwater (Millero, 2016). DOM adsorption to particles has also been reported in estuaries, especially estuaries with high suspended solids loads (Hedges & Keil, 1999; Keil et al., 1997). Therefore, POM formation should occur in any estuaries, but publications have also documented conservative behavior of the organic matter in these systems (Mantoura & Woodward, 1983; Markager et al., 2011). Flocculation mechanism in estuarine mixing has been observed to depend on the drainage basin of the river (Asmala et al., 2013; Sampedro-Avila et al., 2024). Sampedro-Avila et al. (2024; Chapter 2 of the present document) observed that POM from two near subtropical rivers (20 km of each other at the sampling locations) corresponding to basins with different land resulted in different mixing behavior.

In this work, laboratory experiments using prefiltered freshwater from different sources and at different seasons were conducted to better understand the POM formation in estuarine mixing.

3.2 Materials and methods

Freshwater was manually collected from five different freshwater sources of the northern coast of Baja California (Ensenada) and the southern coast of California (San Diego) (Figure 4, Table 2), in acid-washed 5-20 L plastic containers. Surface seawater from the Todos Santos Bay wa aged for about 1 year before the experiments, and deep seawater (950 m) was also used and aged for some experiments. Experimental setup and some analyses were similar to those described in Sampedro-Avila et al. (2014), except for the use of prefiltered water in both end members.

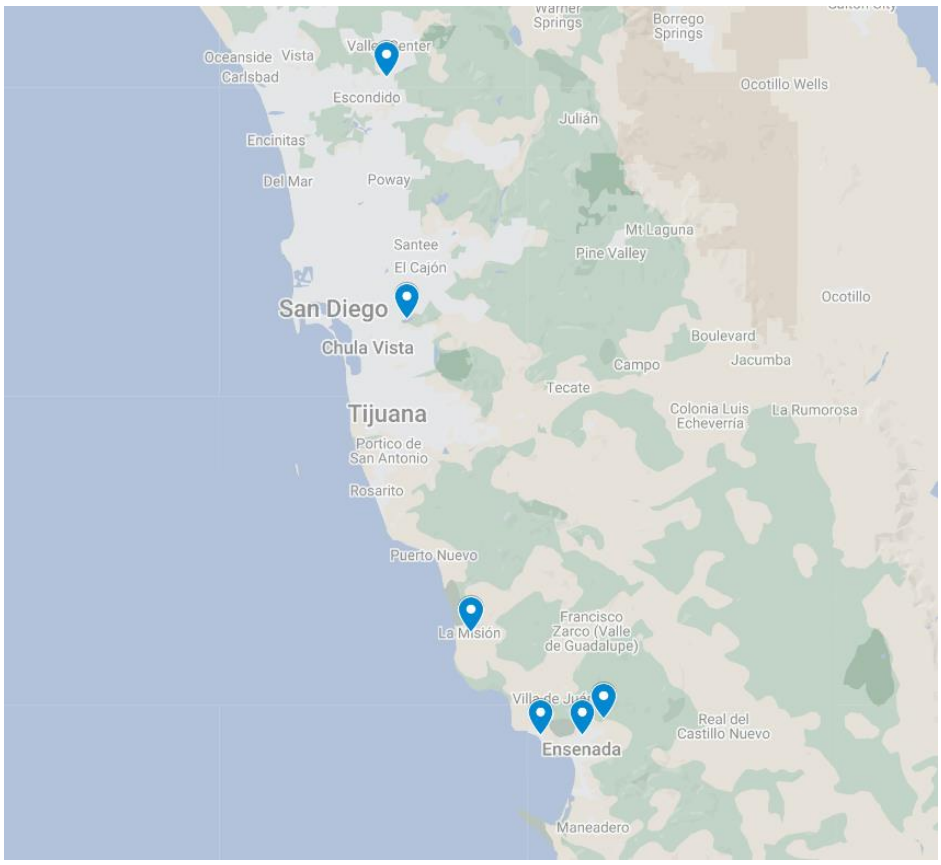

Figure 4. Locations of freshwater sources used for the mixing experiments conducted with prefiltered seawater. Created with Google My Maps.

Briefly, a total of 15 mixing experiments were conducted from August 2018 to April 2022. Water from the two end members were prefiltered with combusted GF/F (Whatman; 450 °C, 4 h) and later mixed at different proportions at room temperature (20-25 °C for different experiments) and low-light conditions. Plastic funnels were previously acid-washed and glassware was precombusted (450 °C, 4 h) before each experiment. Filter samples for elemental analysis (VarioMicro, Elementar) were stored at -20 °C until measuring, and liquid samples for TOC and DOC (VarioTOC, Elementar) were acidified with HCl 6N to reach <2 pH and stored at 4 °C.

Elemental analysis measurements were calibrated with acetanilide. TOC and DOC measurements were calibrated with potassium hydrogen phthalate, and Low Carbon Water and Deep Seawater Reference from Hansell laboratory (University of Miami) were used to verify it. Precision for performed analyses was 5-10%.

Water hardness samples were analyzed immediately after each experiment, using EDTA titration with a micro-burette according to ¨Standard Methods¨ protocol 2340a (APHA et al., 2012). Water temperature, salinity, conductivity, and pH were measured with a glass thermometer, a refractometer, a conductivity meter, and a bench potentiometer, respectively.

Rain precipitation data of the meteorological station of the Ensenada Reservoir were obtained from the national water agency (CONAGUA) website (https://smn.conagua.gob.mx/es/climatologia/informacion-climatologica/informacion-estadistica-climatologica). Accumulated monthly rainfall was calculated from daily data of the meteorological station (Figure 6).

Microsoft Excel 365 was used for these calculations and to generate some figures. Statistical analyses (as described in Sampedro-Avila et al., 2024; $\alpha = 0.05$) and other figures were performed with RStudio software (version 2023.03.1 + 446), using the package *tidyverse* (Wickham et al., 2019) and R base functions.

3.3 Results

TOC and DOC values in all freshwater sources were higher than those in seawater (Figure 5), while electrical conductivity and water hardness were higher in seawater (data not shown). Electrical conductivity and water hardness in the Ensenada Reservoir increased along the studied period with the highest values in November, 2021 (2864 µS cm-1 and 687 mg CaCO3 L-1, respectively). The water level of this reservoir decreased in the studied period (Figure 7). The electrical conductivity and water hardness were probably correlated with rainfall annual cycles (Figure 6). The highest accumulated rainfall ocurred in March 2020 (100 mm), followed by December 2021 (72 mm), and January 2021 (66 mm). La Niña phase of the El Niño-Southern Oscillation (ENSO) caused weather conditions that were drier than average in this region.

POM formation, as observed in by POC concentrations above the mixing line (Figure 5) ocurred after mixing prefiltered seawater with freshwater from four different sources (Sweetwater Reservoir, Ensenada Reservoir, Dixon Reservoir and Cuatro Milpas Stream) in seven laboratory experiment from different dates (Table **2**). POC formation in the Sweetwater Reservoir experiments 24 h after the mixing was higher than i 1 h after mixing (Figure 5b).

Conservative behavior was observed in the experiment with water from La Misión Stream, and in seven experiments from the Ensenada Reservoir (data not shown). POM formation in the Ensenada Reservoir experiments coincided with rainfall peaks, while conservative results ocurred after several months of drought, when electrical conductivity and water hardness had incresed (Figure 6).

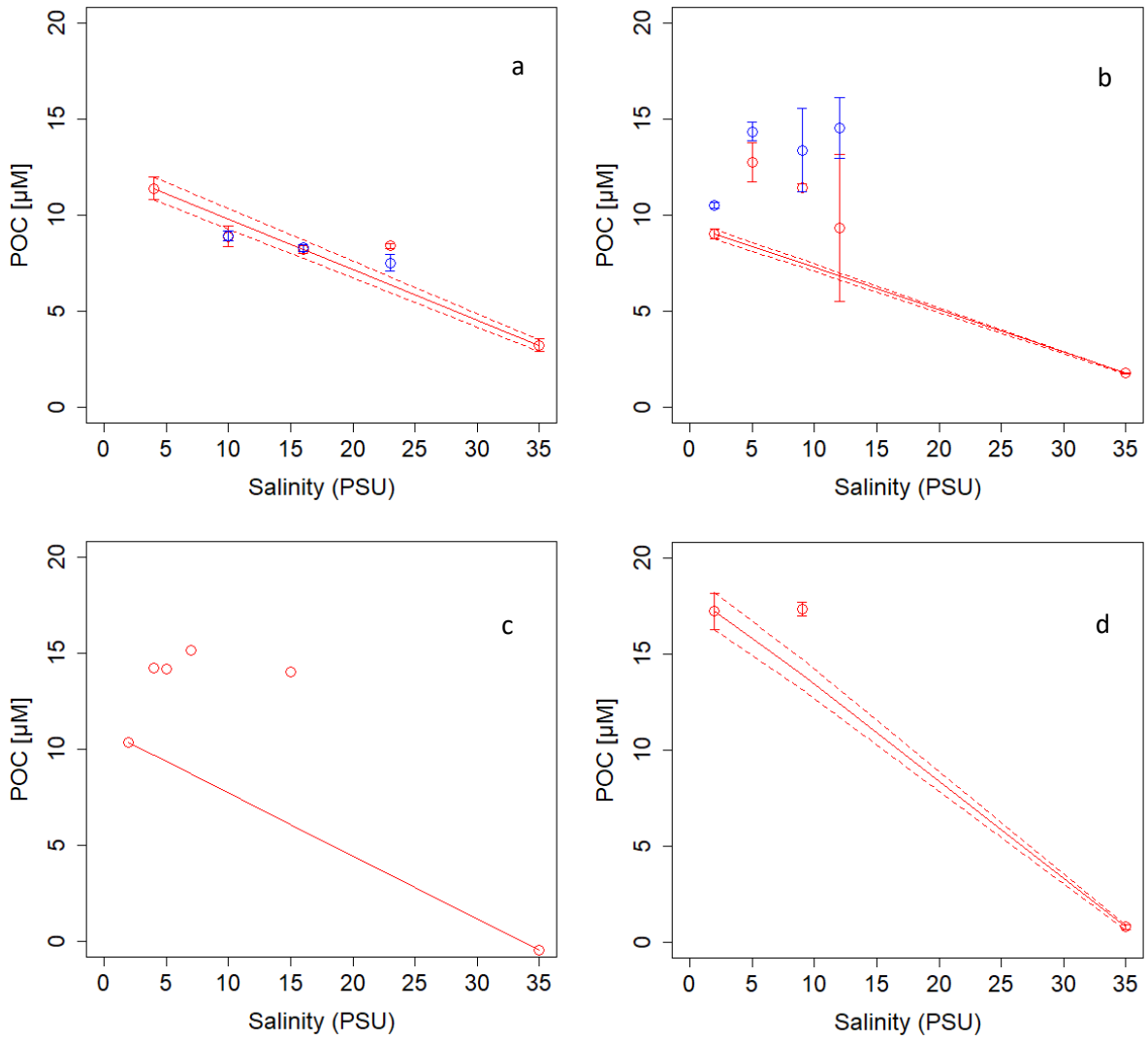

Figure 5. Examples of some conducted mixing experiments with prefiltered water. Particulate organic carbon (POC) in mixed prefiltered seawater with freshwater from the Misión stream (a, Aug-2018), the Sweetwater reservoir (b; Feb-2019), the Ensenada reservoir (c; Mar-2020), and the Cuatro Milpas stream (d; Apr-2022). Red circles corresponded to samples collected 1 h after the mixing simulation, and blue circles were samples collected 24 h after mixing. Error bars and dashed lines represented the standard deviation (n=2).

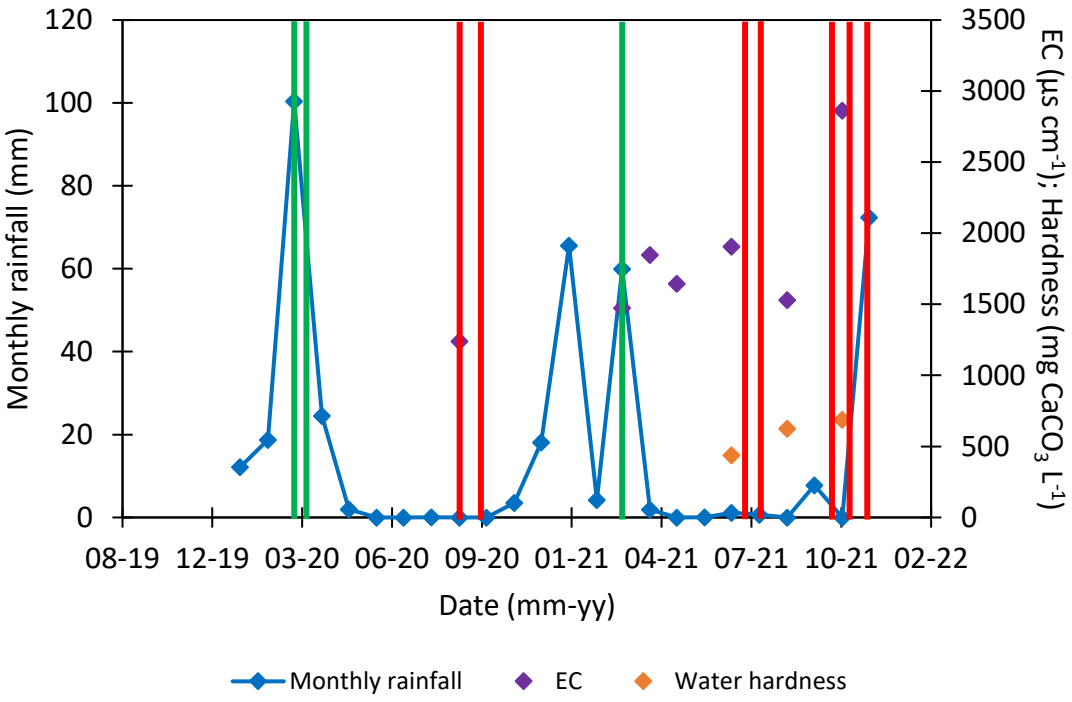

Figure 6. Monthly accumulated rainfall, electrical conductivity (purple) and water hardness (orange) in the Ensenada Reservoir for the studied period (2020-2021). Green vertical lines indicate an experiment where flocculation was observed; red vertical lines indicate conservative behavior in the experiment.

Figure 7. Pictures of the southern wall of the Ensenada Reservoir (¨Presa Emilio López Zamora¨), that documented the water level variation. The orange line indicated the water level observed in March 2020 and marked in the wall. The red arrow indicated a cement permanent structure, as a reference of the water level.

3.4 Discussion

POC formation occurred in seven experiments but a conservative behavior was observed in other eight experiments using prefiltered source water. This pattern was similar to results reported in the literature where either mixing behavior has been reported. Published reports might have differed due to different methodological approaches. Artifact effects could be considered to explain mixing behavior inconsistencies within different authors, but the present results with conservative or non-conservative behavior were obtained with the same experimental set up. Flocculation also ocurred in one of seven experiments in Sampedro-Avila et al. (2024), with a similar protocol but using unfiltered natural river and seawater. These authors conducted two experiments simultaneously with water from two different rivers (Mission and Aransas), and a clear signal of POM increase was observed only in one of them; contamination in those experiments was then unlikely. Natural mechanisms (flocculation and/or adsorption to particles) probably explained then the different mixing results within the present experiments and in the literature.

Another consideration when studying estuarine mixing behavior is the DOM adsorption to glass fiber filters (García-Mendoza, 1994). Adsorbed DOC to the filter was subtracted from the measured POC by using two GF/F filters sequentially (Chaves et al., 2021). It was unexpected that the prefiltered freshwater and seawater end members contained POM (Figure 5), since the prefiltering should have removed all POM. The POM load in the prefiltered endmembers can be explained by POC formation during the prefiltration process due to hydraulic stress (Valdés-Villaverde, 2018). The baseline in the freshwater end member was always higher than in the seawater, probably due to a higher DOC concentration in the freshwater (up to 1,000 µM in the Ensenada reservoir, and and up to 100 µM in the seawater).

The drainage basin of the river end member has been highlighted to determine the mixing behavior of organic matter in its estuarine mixing (Asmala et al., 2013; Sampedro-Avila et al., 2024). The Sweetwater reservoir is mainly fed by freshwater transported from central California to southern California, but also receives a variable portion of water from local rivers. Experiments conducted with natural (non-prefiltered) water collected in April, 2022, from the Sweetwater Reservoir (with a DOC of 1,000 µM) resulted in conservative behavior (data not shown). Moreover, the USGS determined that urbanization in the last decades had caused an increase in pesticides, polynuclear aromatic hydrocarbons (PAHs) and other compounds derived from human activities in this reservoir (Majewski, 2001).

Experiments with natural water from the anthropogenically influenced Aransas River resulted in conservative behavior in two consecutive years, which suggested that organic matter from human activities was not relevant for flocculation. Flocculation with water from the Sweetwater Reservoir might ocurr when terrestrial organic matter loads were transported from distant rivers to this water body.

Table 2. Freshwater sources used for mixing experiments with prefiltered water (Column # was the experiment number), performed analyses and mixing behavior observed. Symbol -- represented that the parameter was not measured for that experiment.

#	Date	Freshwater source	Electrical conductivity ($\mu S\ cm^{-1}$)	Water hardness (mg $CaCO_3$ L^{-1})	DOC decrease or POC increase [μM]	Performed analyses
1	16-ago-18	La Misión Stream	--	--	Conservative	POC
2	16-oct-18	Sweetwater Reservoir	--	--	11	POC
3	06-feb-19	Sweetwater Reservoir	--	--	7	POC
4	12-mar-20	Ensenada Reservoir	--	--	62	DOC, TOC
5	20-mar-20	Ensenada Reservoir	--	--	9	POC
6	08-sep-20	Ensenada Reservoir	1240		Conservative	DOC, TOC
7	19-sep-20	Ensenada Reservoir	--	--	Conservative	DOC, TOC
8	03-mar-21	Ensenada Reservoir	1475	--	104	DOC, TOC
9	08-jul-21	Ensenada Reservoir	1907	438	Conservative	DOC, TOC
10	28-jul-21	Ensenada Reservoir	--	--	Conservative	DOC, TOC
11	17-ago-21	Dixon Reservoir	974	294	56	DOC, TOC
12	12-nov-21	Ensenada Reservoir	2864	687	Conservative	DOC, TOC
13	19-nov-21	Ensenada Reservoir	--	--	Conservative	DOC, TOC
14	01-dic-21	Ensenada Reservoir	--	--	Conservative	DOC, TOC
15	05-abr-22	Cuatro Milpas Stream	1983	722	5	POC

For instance, different drainage basins in the Mission and Aransas River might have caused the flocculation in only one river after sampling the water (Sampedro-Avila et al., 2024). However, flocculation and conservative mixing have ocurred in the same Mission River but in two different years. A combination of the drainage basin character (organic matter composition, cations concentration, etc.) and the seasonal

variations (wet/dry periods) might control the ocurrence or not of flocculation. The streamflow increase effect in the Mission River mixing experiment was interpreted to a higher transport of terrestrial organic matter that depleted δ^{13}C-POC and increased the POC/PON in the flocculated POM (Sampedro-Avila et al., 2024). A similar scenario could have happened in the mixing experiments with the Ensenada Reservoir freshwater. However, increasing patterns in electrical conductivity and water hardness (as indicators of cations concentration) in the reservoir were observed, that could be related to evaporation in dry months (Figure 6).

Higher cations concentration in the freshwater could cause the flocculation of DOM to form POM in the freshwater without addition of seawater. In this case, there would be no DOM with predisposition to flocculate (e.g. terrestrial organic matter) when mixed with seawater. Knowledge of the chemical composition of the flocculants formed in mixing experiments with Ensenada Reservoir freshwater may lead to a better understand its source.

Flocculation observed in a mixing experiment with water from the Dixon Reservoir in August 2021 suggested that the chemical composition of the organic matter and/or water hardness due to the influence of its hydrological basin was relevant. The Dixon reservoir is the northnest freshwater source used for the present experiments. This location was still in the region affected from droughts by La Niña phenomenon in the studied period, but the electrical conductivity and water hardness indicated that cations concentration was lower than the freshwater in other experiments and DOC concentration was 550 µM. The flocculation observed with Dixon reservoir water suggested that the cations concentration of the freshwater was related to the flocculation potential when mixed with seawater.

A map of water hardness distribution in the freshwater of the United States from 1975 indicated that the cations concentration decreased from South to North in the Pacific coast (https://www.usgs.gov/media/images/map-water-hardness-united-states). Flocculation in estuaries of Finland had been frequently reported and could be probably related to a low cations concentation in the river water at that high latitude (Asmala et al., 2013, 2014, 2022). Even if the water hardness of the freshwater was not the only determinant for the flocculation potential of freshwater mixed with seawater, it can still be concluded that the potential for floculation of west-coast freshwater increased with greater latitude.

3.5 Conclusions

Experiments with prefiltered endmembers had the advantage that the results were simpler to interpret and they were more sensitive indicators of the flocculation potential because the baseload of organic and inorganic particles were removed. Therefore, any non-conservative increase in POM had to be the result of DOM flocculation. Physical adsorption of organic matter to the filter surface could be accounted by using double filters. In the future, the analysis of the composition of the organic matter in the mixing experiments would help to have a understanding of the causes and conditions for DOM flocculation in different freshwater sources.

Chapter 4. Evaluation of methods to study flocculation on estuarine mixing and microbial respiration of flocculants

4.1 Introduction

Since the 1970 decade, the behavior of organic matter in estuarine mixing has been studied through the analyses of bulk dissolved or particulate organic matter (Forsgren et al., 1996; Mantoura & Woodward, 1983; Moore et al., 1979; Søndergaard et al., 2003), humic substances (Eckert & Sholkovitz, 1976; Ertel et al., 1986; E. Sholkovitz et al., 1978; E. R. Sholkovitz, 1976) and colored or fluorescent dissolved organic matter (Asmala et al., 2013, 2014; Markager et al., 2011; Wang & Gao, 2022). Flocculation of organic matter has been observed in some works (Asmala et al., 2014; Eckert & Sholkovitz, 1976; Forsgren et al., 1996; Fox, 1983; Furukawa et al., 2014; Ming & Gao, 2022; E. Sholkovitz et al., 1978; E. R. Sholkovitz, 1976; Wang & Gao, 2022). However, some authors have suggested that flocculation on occasion might not have been observed because only about 10% of the bulk DOC had the potential to flocculate (E. R. Sholkovitz, 1976). Contamination and organic matter adsorption need to be ruled out to distinguish this mechanism of POM formation.

Sorption of dissolved organic matter to particles should be considered separate from the flocculation of dissolved organic matter, and might be important in turbid rivers (Hedges & Keil, 1999; Keil et al., 1997). Specific observation of flocculated particles is then important to clear out these different processes that form particulate organic matter. Self-assembly or gel-like particles have been studied in the marine environment (Baltar et al., 2016; Chin et al., 1998; Ding et al., 2007; Orellana et al., 2007; Sun et al., 2018; Verdugo, 2012; Verdugo et al., 2008). Identification and quantification of gels has been approached using a fluorochrome (chlortetracycline hydrochloride, CTC). CTC attaches to the calcium linking the organic molecules forming the gel (Millero, 2016). CTC has been quantified with spectrofluorometers (Baltar et al., 2016; Ding et al., 2007) and flow cytometers (Ding et al., 2007; Orellana & Verdugo, 2003). Observation of CTC with epifluorescent microscope was only mentioned in a published work (Sun et al., 2018) and a PhD dissertation (Jennings, 2017), but their detailed protocol was not provided. Dual staining with fluorochromes to label attached and/or free-living bacteria interacting with the flocculants had not been done and might provide important information on the ecological importance of these particles.

Some bacteria communities might preferentially consume either dissolved or particulate organic matter (Amon & Benner, 1994; Gason & Kirchman, 2018; Jessen et al., 2017; Sivadon et al., 2019; Verdugo, 2012; Woebken et al., 2007), and also select particles with specific composition (Biddanda & Benner, 1997; Findlay & Sinsabaugh, 2003; Thurman, 1985; Wangersky, 1984). Besides of observing the interaction of bacteria with flocculated particles, quantify their aerobic respiration is relevant for the oxygen consumption close to river mouths.

The impacts of the formed flocculants in coastal environments have not been further studied, but particulate organic matter from terrigenous sources has been documented to accumulate in hypoxic zones (also known as 'dead zones') in the northern Gulf of Mexico (Liu & Xue, 2020; Swarzenski et al., 2008), and flocculants are probably composed by terrigenous organic matter (Sampedro-Avila et al., 2024). Hypoxic levels are not tolerated by many different groups of marine organisms and thus impact the coastal ecosystems (Gobler & Baumann, 2016; Vaquer-Sunyer & Duarte, 2008). Oxygen consumption attributed to microbial aerobic respiration is causing an increase in hypoxic zones (Breitburg et al., 2018; Rabalais et al., 2010; Rabalais & Turner, 2019).

4.2 Experimental setup to study flocculation of organic matter from natural and filtered water

Photochemical and biotic processes affect organic matter aggregation and dissolution in estuaries (Hernes & Benner, 2003; Mayer et al., 2009; Orellana & Verdugo, 2003; Wu et al., 2019). Therefore, short (2 h) laboratory experiments were suggested to study the behavior of organic matter in estuarine mixing (Figure **8**). Environmental conditions, as temperature and turbulence, that could be relevant for the flocculation of organic matter (Burns et al., 2019; Chen et al., 2015) were also controlled in these experiments. Briefly, water was collected in acid-washed carboys from a river or freshwater reservoir, and from the coast. Collected water was transported to the laboratory in dim conditions.

Freshwater and seawater were mixed in different proportions and shaken for 20-30 minutes in acid-washed 0.5-1 L bottles (or Erlenmeyer flasks) in dim light conditions and at controlled or stable room temperature (around 18 °C). River and seawater endmembers were treated the same. Two or three replicates were prepared for each mixing proportion and endmember.

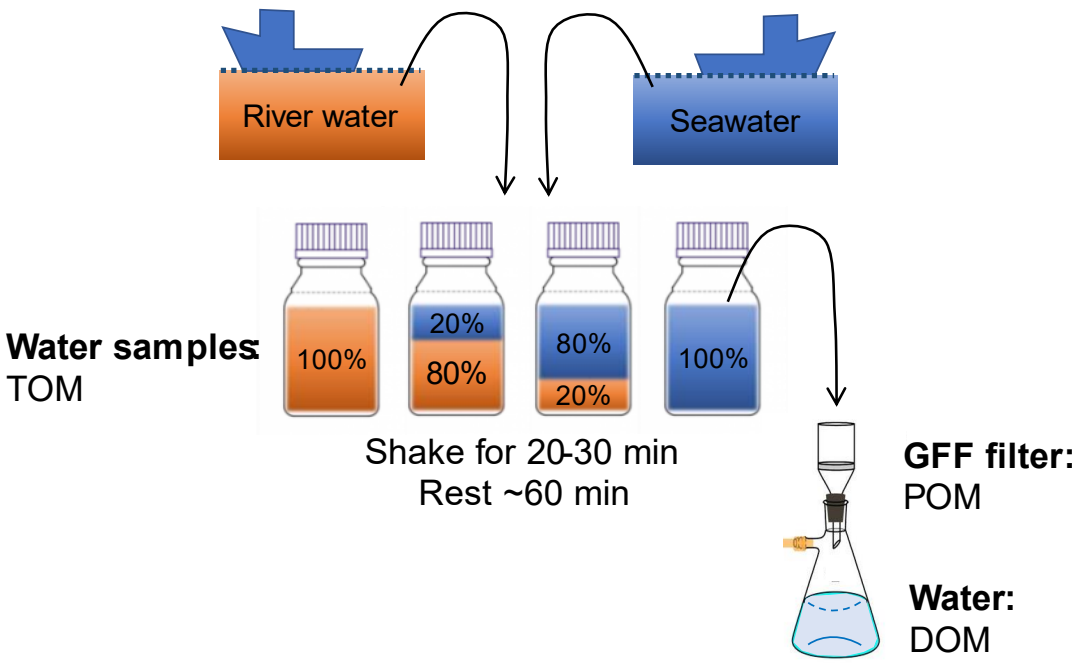

Figure 8. Experimental design to study the mixing behavior of unfiltered riverine dissolved organic matter with seawater in the laboratory.

After 60 minutes of rest, the water from each bottle was individually filtered through combusted GFF filters with combusted glassware and/or acid-washed (10% HCl) plastic funnels. Filters were preserved at -20 °C to later analyze them POM samples for POC, PON, stable isotopes of carbon and nitrogen, and total hydrolyzable amino acids (THAA). The filtered water was also analyzed in some experiments to quantify the dissolved organic carbon and nitrogen (DOC and DON), and the dissolved hydrolyzable amino acids (DHAA). Total organic carbon and nitrogen (TOC and TON) was also analyzed in water samples from the bottles before filtering the mixed water.

Similar experiments were also conducted with prefiltered water (combusted GF/F) to remove the natural POM in the river and seawater (Figure **9**). In this setup, the detected POM after filtration must have been formed exclusively from the flocculation of natural DOM (or sorption) caused by mixing with seawater.

However, POC signal was obtained from the endmembers, which suggested that aggregation of DOM also occurred probably triggered by hydraulic stress (Burns et al., 2019).

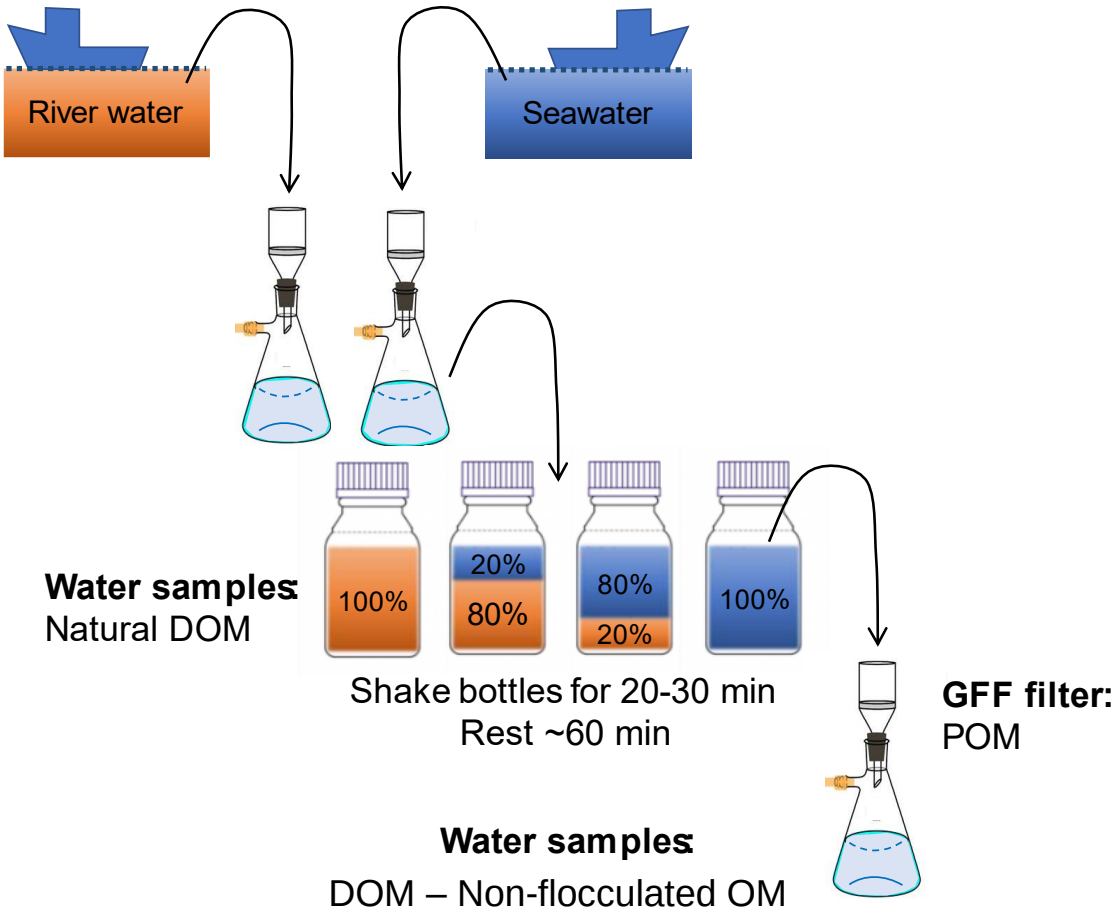

Figure 9. Experimental design to study the mixing behavior of prefiltered dissolved organic matter with seawater in a laboratory.

Sorption of dissolved organic matter to the filter surface was ruled out by one of three different options for each experiment: Two in-line filters (the signal in the top filter was subtracted from the bottom filter), a linear regression of the measured signal with different volumes of the same sample (the intercept in the y-axis was subtracted), and filtering the water for a second time (the signal in the second filtration is subtracted) (Chaves et al., 2021). POM has been observed to be produced as an artifact effect of the hydraulic stress of the filtering, besides of the sorption of DOM, depending on the vacuum pressure (Valdés-Villaverde, 2018). The procedure to subtract this blank signal must be carefully selected then.

The use of a small number of replicates (e.g. duplicates or replicates) to quantify the uncertainty from an experiment could be arguable. The standard deviation of duplicates has been discussed to be underestimated and a modification in its computation was suggested (Synek, 2008). However, standard deviation from replicates in the present work were computed as usual. Significant differences in the graphs of the present file could be biassed, but only the data with a clear pattern were considered to quantify flocculation of organic matter.

4.3 Total, dissolved and particulate organic matter analyses to quantify flocculation

Organic matter amount would be expected to change proportionally to the river or seawater content along a salinity gradient at estuarine mixing (conservative behavior) However, if another process besides of mixing would be involved, the POM or DOM might change, as indicated by POC and DOC in Figure 10 (Swarzenski et al., 2003), respectively. In the laboratory experiments setup suggested in the present work, the only processes that could exclusively cause a non-conservative behavior of POM and DOM (after ruling out contamination and DOC sorption) would be rapid abiotic flocculation/dissolution.

Elemental analysis for POC and PON (often coupled with mass spectrometry for carbon and nitrogen isotopes), and TOC and TON analyses were convenient to quantify flocculation of organic matter in mixing experiments. Carbon and nitrogen isotopes and total hydrolyzable amino acids (with a HPLC with UV detection) were also valuable to provide insights in the formed POM and its source.

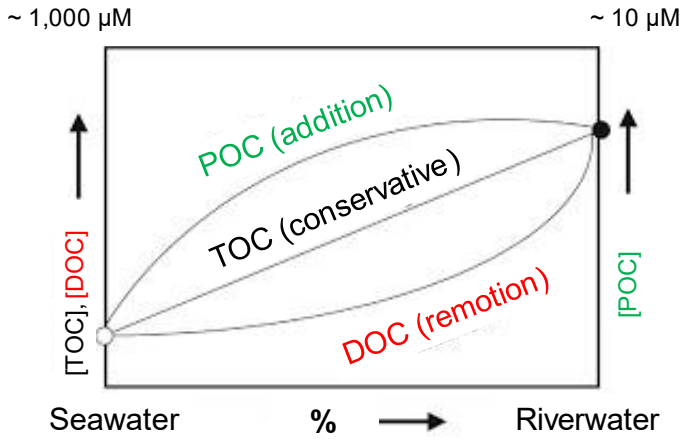

Figure 10: Theorical behavior scenarios of total, dissolved and particulate organic matter (TOC, DOC and POC, respectively) in estuarine mixing. Modified from Swarzenski et al. (2003).

4.4 Characteristics and pretreatment of filters used for the study of flocculation

Glass fiber filters (GF/F, Whatman; AP40, Millipore; GF75, Advantec) were the most adequate to filter the organic matter in the experiments. Even filters which might filter smaller particles than glass fiber filters, but are made of other materials lead more easily to sample contamination. Precombusted glass fiber filters (4 h, 350 °C) prevented the contamination with organic matter. Precombustion has also been documented to decrease the effective pore size of AP40, Millipore (Nayar & Chou, 2003).

Precombusted GF/F filters (Whatman; nominal pore of 0.7 µm) were the most extensively used filters to collect aquatic POM in the related literature. However, GF75 filters (Advantec) have been tried recently because of a smaller nominal pore size (0.3 µm). The transition between dissolved and particulate has been an operational definition based in the used filters (traditionally within 0.45-0.7 µm. Smaller pores would result in smaller particles and a higher amount of material. Evaluating the transition from traditionally used GF/F to GF75 was therefore important. An experiment to compare GF75 and GF/F filters was setup with 300 and 500 mL of surface seawater, and 300 mL of 10% of freshwater from the Ensenada Reservoir +90 % of the seawater (Figure **11**). Retention difference of POC with the two filters was not significant (paired *t test*, $\alpha = 0.05$).

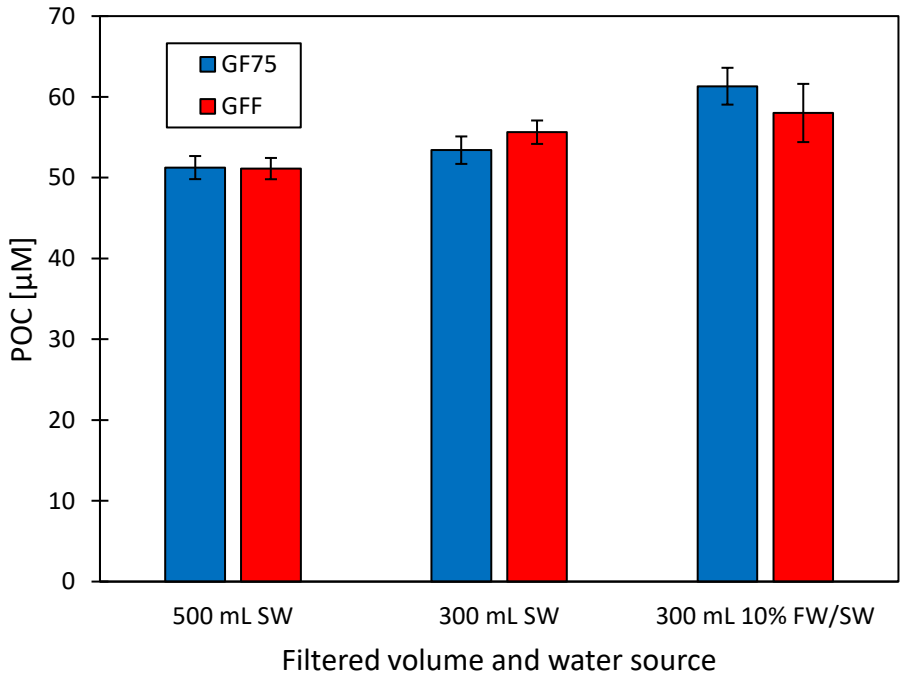

Figure 11. Particulate organic carbon (POC) results from surface seawater, and 10% freshwater + 90% seawater, to evaluate retention amount with GF/F (Whatman) and GF75 (Advantec).

Dissolved organic carbon after filtering with GF/G and GF75 was evaluated for the same purpose on the filtrate of samples of mixed seawater (15%) and freshwater from the Ensenada reservoir (85%) (Figure **12**). The total organic carbon was also measured from the mixed water before filtering, and no different retention of POC between the filters was observed. Bacteria counts in the filtrate water were not significantly different. Another graduate student in the same laboratory demonstrated a higher POC retention with GF/F than AP40 (Millipore) (Valdés-Villaverde, 2018). Moreover, the baseline signal in an elemental analyzer (VarioMicro Cube, Elementar) was analyzed for combusted GF/F and GF75 filters (combusted and non-used) without sample, within a run of 170 samples (Figure **13**). GF/F filter resulted in a lower baseline signal, and more constant along the run.

The present evaluation suggested to continue using GF/F (Whatman) due to the retention efficiency, the signal accuracy and precision, and for a better comparison of results with the literature (Chaves et al., 2021).

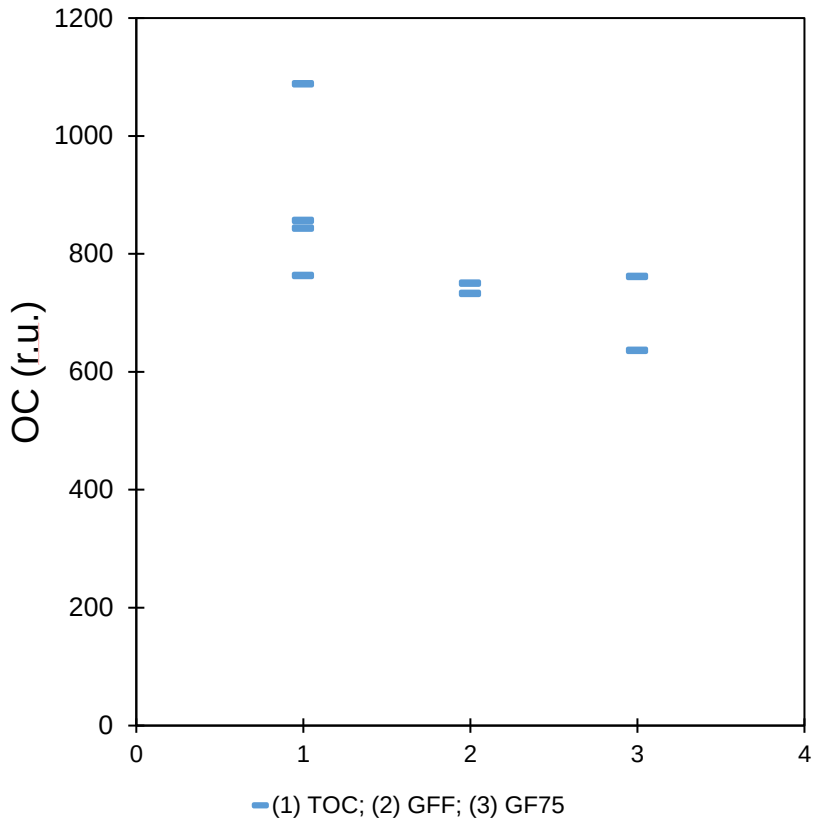

Figure 12. Total organic carbon (TOC), dissolved organic carbon (DOC) after filtering with GF/F, and DOC after filtering with GF75. Seawater (15%) mixed with freshwater (85%) was used to evaluate the POC retention amount with the two different filters.

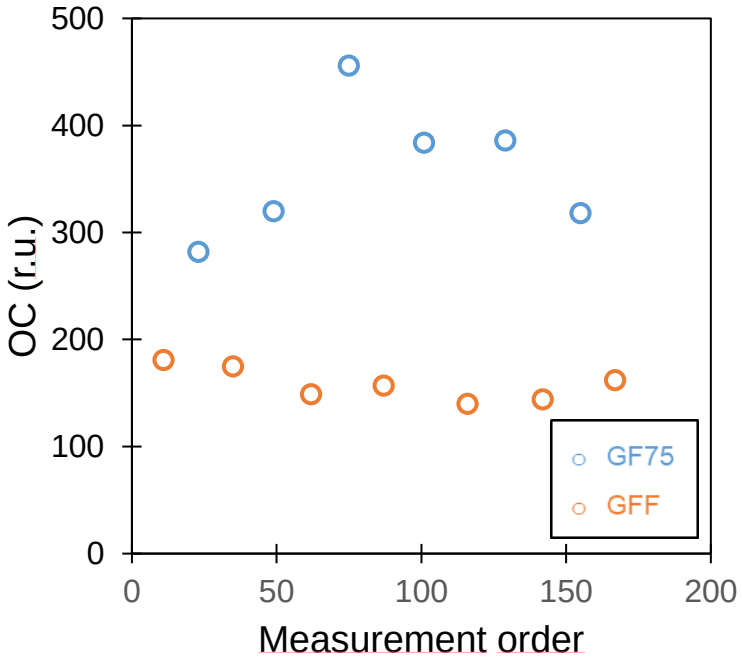

Figure 13. Baseline signal of organic carbon measured along a samples run with elemental analyzer on combusted glass fiber filters.

4.5 Epifluorescence microscopy to observe gel-like flocculants

Chlortetracycline hydrochloride (CTC) is an antibiotic commonly applied for gram-positive bacteria, that has been used also as a fluorescent indicator of Ca^{2+} links that form gel-like particles. CTC interacts with Ca^{2+} links to form fluorescent chelated metals in excitation/emission wavelengths of 400/530 nm and 345/430 nm, but Jennings (2017) recommended to use an emission spectrum of 350-700 nm for spectrofluorometer (Jennings, 2017). This compound does not fluoresce in ultrapure water, and has been used for marine microgels (Baltar et al., 2016; Ding et al., 2007; Orellana et al., 2007), where marine Ca^{2+} concentrations are higher than in river or estuarine water. Therefore, interference with dissolved calcium in mixed water to observe flocculation should not occur.

Briefly, 1-2 mL samples were prefiltered with 8 µm pore size to exclude greater particles (e.g. phytoplankton cells), and 10-20 µL of SYBR Green or DAPI were added (when dual staining was desired) and incubated for 10-15 minutes at dark. Samples stained for bacteria (or samples only prefiltered) were filtered with 0.2 µm black polycarbonate membranes (Nucleopore) at controlled vacuum pressure (10 kPa). 100 µL of CTC were later added to the filters and incubated for 15 minutes in the dark. Filters were later mounted in slides and antifading solution was used to observe with a Axioskope II Plus (Carl Zeiss)

with different excitation and emission filters (e.g. 422-432/593 nm). A CCD camera (Clara, Andor) and a Z controller were used to take images of different depths. Stacks and composite images were performed with opensource software ImageJ (FIJI).

Optical cross-talk of CTC occurred when dual staining with DAPI or SYBR Green to observe associated bacteria (Figure **14**). Non-amplified fluorescence *in situ* hybridization (FISH) (Cruz-López & Maske, 2015) was recommended to be implemented in combination with CTC, using different optical filters to observe groups of bacteria and their niche in the samples.

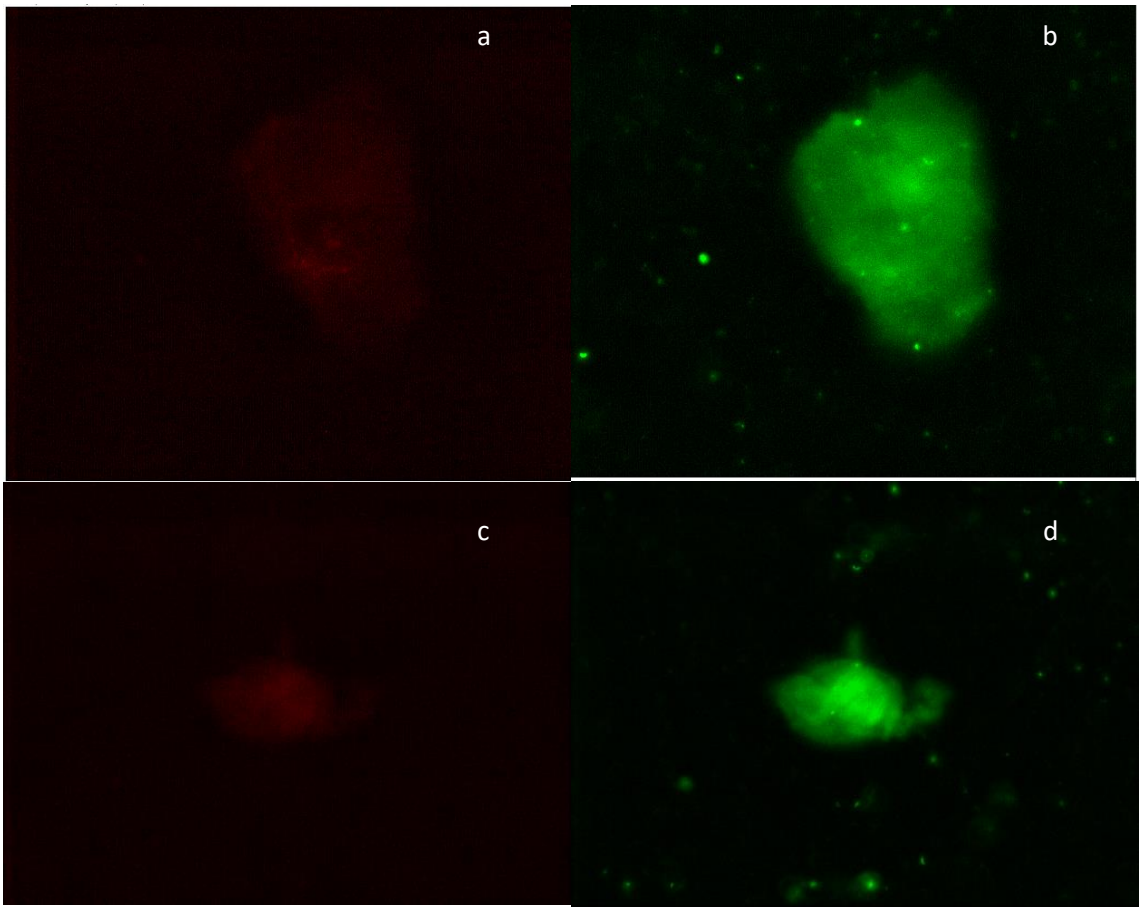

Figure 14. Dual staining for flocculants (a, c; CTC at 422-432/593 nm) and associated bacteria (b, d; SYBR Green at 450-490/515 nm) in mixed water (80% freshwater+20% seawater) observed in an epifluorescent microscope (1000x). Cross-talk of fluorescence emission is observed in b and d.

Jennings (2017) suggested to complement CTC observations with TOC or TEPs analyses. Staining with Alcian Blue could be used to observe TEPs in light microscopy (Figure **15**). Some areas of the observed particles were coincident between the two staining reagents. Similar observations were reported by Jennings (2017). Gel-like particles showed “stickiness” properties that cause entanglement with other

organic and inorganic particles (Santschi et al., 2021), therefore a combination of different chemical compositions might occur in a single aggregate.

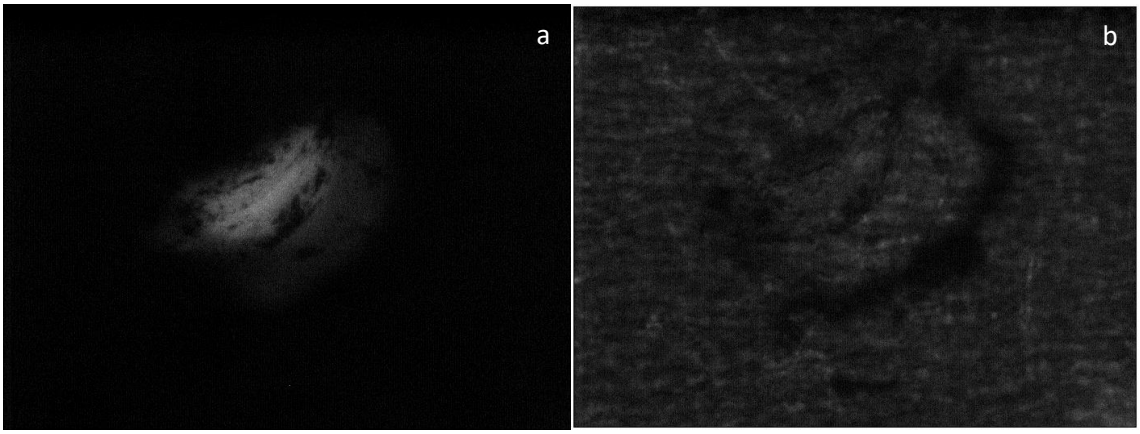

Figure 15. Dual staining for flocculants (a; CTC at 422-432/593 nm) and transparent exopolymer particles (TEPs, b; Alcian Blue with transmitted light) in prefiltered Thalassiossira weissflogii culture (8 µm polycarbonate membrane) observed in an epifluorescence microscope (1,000x). Blurred background in b corresponds to the filter pores.

Chlortetracycline solutions in distilled water showed fluorescent matrices (fluorescent debris) on a few occasions. The following recommendations were concluded to prevent CTC noise signal:

- Prepare a stock solution (100 µM) with recently produced distilled or ultrapure water and store at -20 C for later samples preparation.
- Adjust the stock solution to pH 8 before storing at -20 C, and check the pH before preparing samples.
- Prefilter working solution (0.2 µm) before staining samples.
- Observe a filter only with an aliquot of the working solution, and another one with distilled or ultrapure water, as blanks.
- Observe a sample without adding chlortetracycline, to check for organic matter autofluorescence.
- When dual staining is desired, observe another subsample only with DAPI or SYBR green.

4.6 Oxygen consumption to estimate respiration rates and lability of flocculants

Closed mixed water incubations resulted in higher oxygen consumption rates (7 µM h^{-1}) at 100% of seawater collected offshore in the Todos Sants Bay (salinity 35) and 80% of seawater + 20% of freshwater

from upstream the Ensenada reservoir (salinity 28.4), while the bottles with 100% of freshwater (salinity 2) had the lowest consumption rates (1 µM h^{-1}) of the experiment (Figure **16**). Higher bacteria abundances were obtained with epifluorescence microscopy from bottles with salinity 35 (0.93 x10^6 cells mL^{-1}) and salinity 28.4 (0.70 x10^6 cells mL^{-1}), than salinity 2 (0.30 x10^6 cells mL^{-1}). Conversely, lower DOC and TOC values were analyzed at salinity 35 (74 µM of DOC and 97 µM of TOC) and 28.4 (237 µM of DOC and 251 µM of TOC than at salinity 2 (754 µM of DOC and 755 µM of TOC). Probably, higher bacteria abundance in seawater caused the higher oxygen consumption in seawater.

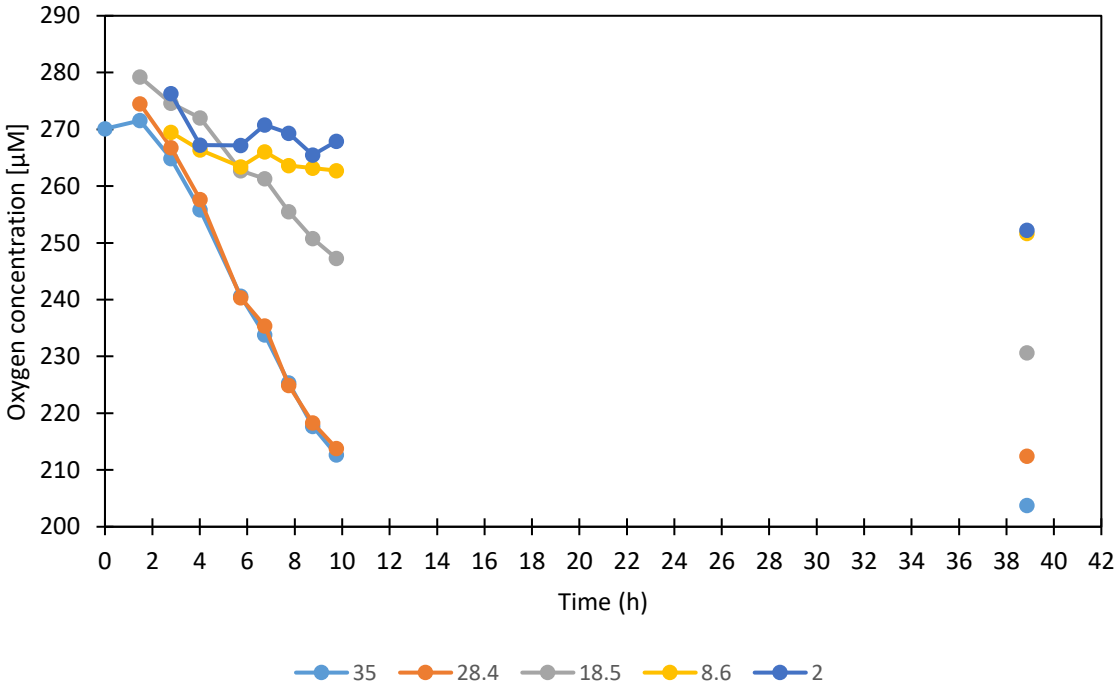

Figure 16. Dissolved oxygen concentration in closed mixed water incubations, measured with PyroScience optodes in time spans from 1 to 29 h. Salinity values resulted from the mixing are labeled in the color scale.

4.7 Calcium removal of hard water sources to understand its effect on flocculation

High cations concentration in freshwater might promote flocculation of dissolved organic matter before being mixed with seawater. To study the mechanism of flocculation it was planned to reduce the cations concentration (Ca^{2+}). EDTA was assessed to chelate this cation to reduce its availability, but POC

concentration increased proportionally to the concentration of EDTA added, contaminating the sample (Figure **17**). Amberlite IR120, an ion exchange resin, was later evaluated to reduce dissolved calcium in the same water.

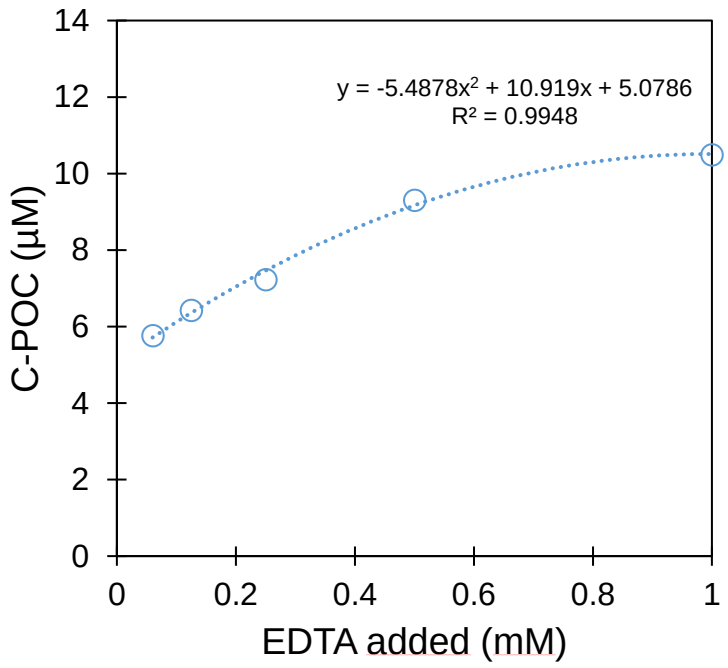

Figure 17. Particulate organic carbon concentration (C-POC) in function of the amount of EDTA added to prefiltered freshwater from the Ensenada reservoir. Measured data were fitted to a binomial curve (dashed line).

The resin successfully reduced calcium concentration (indicated by water hardness), but also increased sodium concentration in the freshwater as indicated by conductivity (Figure 18). Sodium ions have been documented to reduce TEPs formation (indicated as Na^{+}/Ca^{2+} ratio), by interacting with its precursors (Meng & Liu, 2016). However, DOC contamination was detected in some experiments even after removing the resin used to treat the freshwater.

Tests were conducted for rinsing the resin with distilled water at room or warm temperature, and sequentially with acetone (90%) and distilled water, before treating freshwater samples. No difference in samples contamination was observed when using distilled water with different temperature to rinse the resin. The rinsing with acetone visually weathered the resin, which could alter the organic matter composition of the later treated water, if not also its concentration.

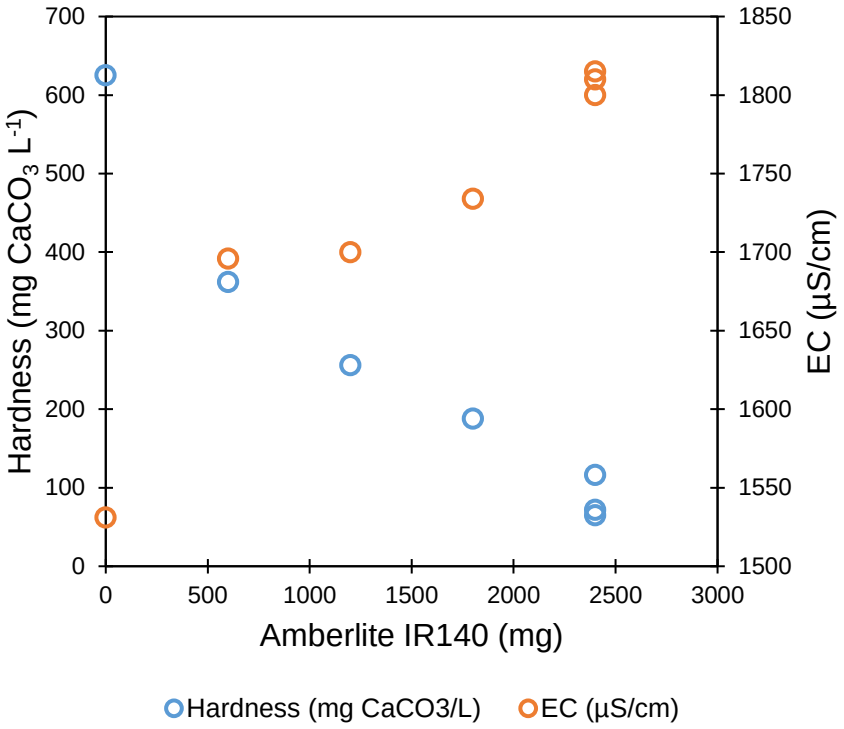

Figure 18. Water hardness (blue) and electrical conductivity (orange) measured after adding ion exchange resin Amberlite IR120 to freshwater of the Ensenada reservoir.

The resin in the distilled water was systematically stirred in a shaker table or in a rolling bottle, and later removed with a 20 or 350 µm mesh. About 100 and 200 µM of sample contamination was reduced when previously stirring the resin in distilled water in a shaker table and in a rolling bottle, respectively. Additional 100 µM contamination was reduced when separating the resin from the rinse water with a 20 µm mesh, instead of the 350 µm mesh. An effective calcium reduction protocol for mixing experiments has not been completely developed yet.

Chapter 5. General conclusions

Flocculation of organic matter in estuarine mixing is a mechanism that is expected to influence significantly the estuarine and coastal ecology, but the flocculation process is not well understood. Flocculation is irregularly observed and the control mechanisms of the flocculation process in nature have not been elucidated. Results from the present work suggested that an increase of rainfall in the drainage basin of the river might promote flocculation, either by a higher input of terrestrial dissolved organic matter (DOM), or by lower cations concentration in the freshwater that allow flocculants precursors to stay in the dissolved phase until estuarine mixing.

Challenges to study flocculation of organic matter in estuarine mixing include the presence of other abiotic and biotic mechanisms that affect this organic matter (e.g. consumption, production, dissolution, adsorption, photooxidation). Laboratory experiments enable to focus on flocculation though conducting short (a few hours) simulations in controlled conditions (e.g. temperature, light, hydraulic stress). Other technical considerations might be relevant to quantify the amount of organic matter flocculated, as filter type, filtration vacuum pressure, excitation and emission filters for epifluorescence microscopy, etc. Protocols to study flocculation and the oxidation of the formed particulate organic matter (POM) still need to be further developed.

Bibliography

Amon, R. M. W., & Benner, R. (1994). Rapid cycling of high-molecular-weight dissolved organic matter in the ocean. *Nature*, *369*(6481), 549–552. https://doi.org/10.1038/369549a0

Anderson, D. (2007). The ecology and oceanography of harmful algal blooms: multidisciplinary approaches to research and management. *IOC Technical Series*, *June*, 38. https://doi.org/IOC/2007/TS/74

APHA, AWAA, & WEF. (2012). *Standard Methods for the Examination of Water and Wastewater* (E. W. Rice, A. B. Baird, A. D. Eaton, & L. S. Clesceri, Eds.; 22nd ed.). American Public Health Association (APHA).

Artemev, V. E. (1996). *Geochemistry of organic matter in river-sea systems*. Springer https://doi.org/10.1007/978-94-009-1681-4

Asmala, E., Autio, R., Kaartokallio, H., Pitkänen, L., Stedmon, C. A., & Thomas, D. N. (2013). Bioavailability of riverine dissolved organic matter in three Baltic Sea estuaries and the effect of catchment land use. *Biogeosciences*, *10*(11), 6969–6986. https://doi.org/10.5194/bg-10-6969-2013

Asmala, E., Bowers, D. G., Autio, R., Kaartokallio, H., & Thomas, D. N. (2014). Qualitative changes of riverine dissolved organic matter at low salinities due to flocculation. *Journal of Geophysical Research G: Biogeosciences*, *119*(10), 1919–1933. https://doi.org/10.1002/2014JG002722

Asmala, E., Virtasalo, J. J., Scheinin, M., Newton, S., & Jilbert, T. (2022). Role of particle dynamics in processing of terrestrial nitrogen and phosphorus in the estuarine mixing zone. *Limnology and Oceanography*, *67*(1), 1–12. https://doi.org/10.1002/lno.11961

Baltar, F., Currie, K., Meyer, M., & Verdugo, P. (2016). Proportion of marine organic carbon present in self-assembled gels along the subtropical front and its increase in response to reduced pH. *Marine Chemistry*, *184*, 53–59. https://doi.org/10.1016/j.marchem.2016.05.014

Benner, R. (1991). Ultra-Filtration for the Concentration of Bacteria, Viruses, and Dissolved Organic Matter. In *Geophysical Monograph Series* (pp. 181–185). https://doi.org/10.1029/GM063p0181

Benner, R., & Opsahl, S. (2001). Molecular indicators of the sources and transformations of dissolved organic matter in the Mississippi river plume. *Organic Geochemistry*, *32*(4), 597–611. https://doi.org/10.1016/S0146-6380(00)00197-2

Bianchi, T. S. (2007). *Biogeochemistry of Estuaries*. Oxford University Press.

Biddanda, B., & Benner, R. (1997). Carbon, nitrogen, and carbohydrate fluxes during the production of particulate and dissolved organic matter by marine phytoplankton. *Limnology and Oceanography*, *42*(3), 506–518. https://doi.org/10.4319/lo.1997.42.3.0506

Breitburg, D., Levin, L. A., Oschlies, A., Grégoire, M., Chavez, F. P., Conley, D. J., Garçon, V., Gilbert, D., Gutiérrez, D., Isensee, K., Jacinto, G. S., Limburg, K. E., Montes, I., Naqvi, S. W. A., Pitcher, G. C., Rabalais, N. N., Roman, M. R., Rose, K. A., Seibel, B. A., … Zhang, J. (2018). Declining oxygen

in the global ocean and coastal waters. *Science*, *359*(6371). https://doi.org/10.1126/science.aam7240

Burns, W. G., Marchetti, A., & Ziervogel, K. (2019). Enhanced formation of transparent exopolymer particles (TEP) under turbulence during phytoplankton growth. *Journal of Plankton Research*, *41*(3), 349–361. https://doi.org/10.1093/plankt/fbz018

Cai, Y., Shim, M. J., Guo, L., & Shiller, A. (2016). Floodplain influence on carbon speciation and fluxes from the lower Pearl River, Mississippi. *Geochimica et Cosmochimica Acta*, *186*, 189–206. https://doi.org/10.1016/j.gca.2016.05.007

Cao, X., Aiken, G. R., Butler, K. D., Huntington, T. G., Balch, W. M., Mao, J., & Schmidt-Rohr, K. (2018). Evidence for major input of riverine organic matter into the ocean. *Organic Geochemistry*, *116*, 62–76. https://doi.org/10.1016/j.orggeochem.2017.11.001

Chanton, J. P., & Lewis, F. G. (1999). Plankton and dissolved inorganic carbon isotopic composition in a river-dominated estuary: Apalachicola Bay, Florida. *Estuaries*, *22*(3), 575–583. https://doi.org/10.2307/1353045

Chaves, J. E., Cetini, I., Olmo, G. D., Estapa, M., Gardner, W., Graff, J. R., Hernes, P., Lam, P. J., Liu, Z., Lomas, M. W., Novak, M. G., Turnewitsch, R., Werdell, P. J., & Westberry, T. K. (2021). Particulate Organic Matter Sampling and Measurement Protocols: Consensus Towards Future Ocean Color Missions. *IOCCG Ocean Optics and Biogeochemistry Protocols for Satellite Ocean Colour Sensor Validation*, *6*(August).

Chen, C. S., Anaya, J. M., Chen, E. Y. T., Farr, E., & Chin, W. C. (2015). Ocean Warming-Acidification Synergism Undermines Dissolved Organic Matter Assembly. *PLoS ONE*, *10*(2), 1–10. https://doi.org/10.1371/journal.pone.0118300

Chenar, S. S., Karbassi, A., Zaker, N. H., & Ghazban, F. (2013). Electroflocculation of Metals during Estuarine Mixing (Caspian Sea). *Journal of Coastal Research*, *289*(4), 847–854. https://doi.org/10.2112/JCOASTRES-D-11-00224.1

Chin, W. C., Orellana, M. V., & Verdugo, P. (1998). Spontaneous assembly of marine dissolved organic matter into polymer gels. *Nature*, *391*(March), 568–572. https://doi.org/10.1038/nature02371.1.

Cisternas-Novoa, C., Lee, C., & Engel, A. (2014). A semi-quantitative spectrophotometric, dye-binding assay for determination of Coomassie Blue stainable particles. *Limnology and Oceanography: Methods*, *12*(AUG), 604–616. https://doi.org/10.4319/lom.2014.12.604

Coplen, T. B. (1996). New guidelines for reporting stable hydrogen, carbon, and oxygen isotope-ratio data. *Geochimica et Cosmochimica Acta*, *60*(17), 3359–3360. https://doi.org/10.1016/0016-7037(96)00263-3

Cruz-López, R., & Maske, H. (2015). A non-amplified FISH protocol to identify simultaneously different bacterial groups attached to eukaryotic phytoplankton. *Journal of Applied Phycology*, *27*(2), 797–804. https://doi.org/10.1007/s10811-014-0379-2

Dauwe, B., Middelburg, J. J., Herman, P. M. J., & Heip, C. H. R. (1999). Linking diagenetic alteration of amino acids and bulk organic matter reactivity. *Limnology and Oceanography*, *44*(7), 1809–1814. https://doi.org/10.4319/lo.1999.44.7.1809

Dawson, T. E., Mambelli, S., Plamboeck, A. H., Templer, P. H., & Tu, K. P. (2002). Stable isotopes in plant ecology. *Annual Review of Ecology and Systematics*, *33*, 507–559. https://doi.org/10.1146/annurev.ecolsys.33.020602.095451

Diaz, R. J., & Rosenberg, R. (2008). Spreading dead zones and consequences for marine ecosystems. *Science*, *321*(5891), 926–929. https://doi.org/10.1126/science.1156401

Ding, Y. X., Chin, W. C., & Verdugo, P. (2007). Development of a fluorescence quenching assay to measure the fraction of organic carbon present in self-assembled gels in seawater. *Marine Chemistry*, *106*(3–4), 456–462. https://doi.org/10.1016/j.marchem.2007.04.005

Droppo, I., Jeffries, D., Jaskot, C., & Backus, S. (1998). *The Prevalence of Freshwater Flocculation in Cold Regions: A Case Study from the Mackenzie River Delta, Northwest Territories, Canada*. *51*(2), 155–164.

Eckert, J. M., & Sholkovitz, E. R. (1976). The flocculation of iron, aluminium and humates from river water by electrolytes. *Geochimica et Cosmochimica Acta*, *40*(7), 847–848. https://doi.org/10.1016/0016-7037(76)90036-3

Ertel, J. R., Hedges, J. I., Devol, A. H., Richey, J. E., & Ribeiro, M. de N. G. (1986). Dissolved humic substances of the Amazon River system. *Limnology and Oceanography*, *31*(4), 739–754. https://doi.org/10.4319/lo.1986.31.4.0739

Findlay, S. E. G., & Sinsabaugh, R. L. (2003). *Aquatic Ecosystems. Interactivity of Dissolved Organic Matter*. Academic Press.

Forsgren, G., Jansson, M., & Nilsson, P. (1996). Aggregation and sedimentation of iron, phosphorus and organic carbon in experimental mixtures of freshwater and estuarine water. *Estuarine, Coastal and Shelf Science*, *43*(2), 259–268. https://doi.org/10.1006/ecss.1996.0068

Fox, L. E. (1983). The removal of dissolved humic acid during estuarine mixing. *Estuarine, Coastal and Shelf Science*, *16*(4), 431–440. https://doi.org/10.1016/0272-7714(83)90104-X

Fry, B. (2006). Stable Isotope Ecology. In *Libro: Vol. XII*. Springer. https://doi.org/10.1007/0-387-33745-8

Furukawa, Y., Reed, A. H., & Zhang, G. (2014). Effect of organic matter on estuarine flocculation: A laboratory study using montmorillonite, humic acid, xanthan gum, guar gum and natural estuarine flocs. *Geochemical Transactions*, *15*(1), 1–9. https://doi.org/10.1186/1467-4866-15-1

García-Mendoza, E. (1994). *Fluorescencia natural y productividad primaria en el Pacífico mexicano*. [Master in Science Thesis, Centro de Investigación Científica y de Educación Superior de Ensenada, Baja California]. https://cicese.repositorioinstitucional.mx/jspui/handle/1007/3118

Gason, J. M., & Kirchman, D. L. (2018). Microbial Ecology of the Oceans. In *John Wiley & Sons, Inc. All* (3rd ed.). John Wiley & Sons.

Gobler, C. J., & Baumann, H. (2016). Hypoxia and acidification in ocean ecosystems: Coupled dynamics and effects on marine life. *Biology Letters*, *12*(5). https://doi.org/10.1098/rsbl.2015.0976

Gregory, J., & O'Melia, C. R. (1989). Fundamentals of flocculation. *Critical Reviews in Environmental Control*, *19*(3), 185–230. https://doi.org/10.1080/10643388909388365

Guadayol, Ò., Peters, F., Stiansen, J. E., Marrasé, C., & Lohrmann, A. (2009). Evaluation of oscillating grids and orbital shakers as means to generate isotropic and homogeneous small-scale turbulence in laboratory enclosures commonly used in plankton studies. *Limnology and Oceanography: Methods*, *7*(4), 287–303. https://doi.org/10.4319/lom.2009.7.287

Hallegraeff, G. M. (1993). Harmful algal blooms in the Australian region. *Marine Pollution Bulletin*, *25*, 186–190. https://doi.org/10.1016/0025-326X(92)90223-S

Han, H., Feng, Y., Chen, J., Xie, Q., Chen, S., Sheng, M., Zhong, S., Wei, W., Su, S., & Fu, P. (2022). Acidification impacts on the molecular composition of dissolved organic matter revealed by FT-ICR MS. *Science of the Total Environment*, *805*, 150284. https://doi.org/10.1016/j.scitotenv.2021.150284

Hansell, D. A., & Carlson, C. A. (2015). Biogeochemistry of Marine Dissolved Organic Matter. In *Biogeochemistry of Marine Dissolved Organic Matter* (pp. i–ii). Elsevier. https://doi.org/10.1016/B978-0-12-405940-5.09993-3

Harvey, H. R., & Mannino, A. (2001). The chemical composition and cycling of particulate and macromolecular dissolved organic matter in temperate estuaries as revealed by molecular organic tracers. *Organic Geochemistry*, *32*(4), 527–542. https://doi.org/10.1016/S0146-6380(00)00193-5

Hedges, J. I. (1992). Global biogeochemical cycles: progress and problems. *Marine Chemistry*, *39*(1–3), 67–93. https://doi.org/10.1016/0304-4203(92)90096-S

Hedges, J. I., & Keil, R. G. (1999). Organic geochemical perspectives on estuarine processes: Sorption reactions and consequences. *Marine Chemistry*, *65*(1–2), 55–65. https://doi.org/10.1016/S0304-4203(99)00010-9

Hedges, J. I., & Stern, J. H. (1984). Carbon and nitrogen determinations of carbonate-containing solids. *Limnology and Oceanography*, *29*(3), 657–663. https://doi.org/10.4319/lo.1984.29.3.0657

Hernes, P. J., & Benner, R. (2003). Photochemical and microbial degradation of dissolved lignin phenols: Implications for the fate of terrigenous dissolved organic matter in marine environments. *Journal of Geophysical Research: Oceans*, *108*(9). https://doi.org/10.1029/2002jc001421

Hodgkin, E. P., & Lenanton, R. C. (1981). Estuaries and Coastal Lagoons of South Western Australia. In *Estuaries and Nutrients* (pp. 307–321). Humana Press. https://doi.org/10.1007/978-1-4612-5826-1_14

Hoyle, J., Elderfield, H., Gledhill, A., & Greaves, M. (1984). The behaviour of the rare earth elements during mixing of river and sea waters. *Geochimica et Cosmochimica Acta*, *48*(1), 143–149. https://doi.org/10.1016/0016-7037(84)90356-9

Jennings, M. K. (2017). *Analytical Improvements for Assessing Dissolved Organic Carbon Concentrations and Dynamics in the Ocean* [Doctorate Dissertation, University of Miami]. https://scholarlyrepository.miami.edu/oa_dissertations/1895%0AThis

Jessen, G. L., Lichtschlag, A., Ramette, A., Pantoja, S., Rossel, P. E., Schubert, C. J., Struck, U., & Boetius, A. (2017). Hypoxia causes preservation of labile organic matter and changes seafloor microbial community composition (Black Sea). *Science Advances*, *3*(2). https://doi.org/10.1126/sciadv.1601897

Karbassi, A. R., & Heidari, M. (2015). An investigation on role of salinity, pH and DO on heavy metals elimination throughout estuarial mixture. *Global Journal of Environmental Science and Management*, *1*(1), 41–46. https://doi.org/10.7508/gjesm.2015.01.004

Karbassi, A. R., Heidari, M., Vaezi, A. R., Samani, A. R. V., Fakhraee, M., & Heidari, F. (2014). *Effect of pH and salinity on flocculation process of heavy metals during mixing of Aras River water with Caspian Sea water*. 457–465. https://doi.org/10.1007/s12665-013-2965-z

Keil, R. G., Mayer, L. M., Quay, P. D., Richey, J. E., & Hedges, J. I. (1997). Loss of organic matter from riverine particles in deltas. *Geochimica et Cosmochimica Acta*, *61*(7), 1507–1511. https://doi.org/10.1016/S0016-7037(97)00044-6

Kranck, K. (1984). The Role Of Flocculation in the Filtering of Particulate Matter in Estuaries. In *The Estuary As a Filter* (pp. 159–175). Elsevier. https://doi.org/10.1016/B978-0-12-405070-9.50014-1

Kritee, K., Sigman, D. M., Granger, J., Ward, B. B., Jayakumar, A., & Deutsch, C. (2012). Reduced isotope fractionation by denitrification under conditions relevant to the ocean. *Geochimica et Cosmochimica Acta*, *92*, 243–259. https://doi.org/10.1016/j.gca.2012.05.020

Kuznetsova, M., & Lee, C. (2002). Dissolved free and combined amino acids in nearshore seawater, sea surface microlayers and foams: Influence of extracellular hydrolysis. *Aquatic Sciences*, *64*(3), 252–268. https://doi.org/10.1007/s00027-002-8070-0

Lebreton, B., Beseres Pollack, J., Blomberg, B., Palmer, T. A., Adams, L., Guillou, G., & Montagna, P. A. (2016). Origin, composition and quality of suspended particulate organic matter in relation to freshwater inflow in a South Texas estuary. *Estuarine, Coastal and Shelf Science*, *170*, 70–82. https://doi.org/10.1016/j.ecss.2015.12.024

Lee, C., Wakeham, S. G., & I. Hedges, J. (2000). Composition and flux of particulate amino acids and chloropigments in equatorial Pacific seawater and sediments. *Deep Sea Research Part I: Oceanographic Research Papers*, *47*(8), 1535–1568. https://doi.org/10.1016/S0967-0637(99)00116-8

Lee, S. A., Kim, T. H., & Kim, G. (2020). Tracing terrestrial versus marine sources of dissolved organic carbon in a coastal bay using stable carbon isotopes. *Biogeosciences*, *17*(1), 135–144. https://doi.org/10.5194/bg-17-135-2020

Li, X., Liu, Z., Chen, W., Wang, L., He, B., & Wu, K. (2018). Production and Transformation of Dissolved and Particulate Organic Matter as Indicated by Amino Acids in the Pearl River Estuary, China. *Journal of Geophysical Research: Biogeosciences*, *123*(12), 3523–3537. https://doi.org/10.1029/2018JG004690

Li, Y., Song, G., Massicotte, P., Yang, F., Li, R., & Xie, H. (2018). Distribution, seasonality, optical characteristics, and fluxes of dissolved organic matter (DOM) in the Pearl River (Zhujiang) estuary, China. *Biogeosciences*, *October*. https://doi.org/https://doi.org/10.5194/bg-2018-403

Liu, Z., & Xue, J. (2020). The Lability and Source of Particulate Organic Matter in the Northern Gulf of Mexico Hypoxic Zone. *Journal of Geophysical Research: Biogeosciences*, *125*(9). https://doi.org/10.1029/2020JG005653

Lohse, L., Kloosterhuis, R. T., De Stigter, H. C., Helder, W., Van Raaphorst, W., & Van Weering, T. C. E. (2000). Carbonate removal by acidification causes loss of nitrogenous compounds in continental margin sediments. *Marine Chemistry*, *69*(3–4), 193–201. https://doi.org/10.1016/S0304-4203(99)00105-X

Lu, K., & Liu, Z. (2019). Molecular Level Analysis Reveals Changes in Chemical Composition of Dissolved Organic Matter From South Texas Rivers After High Flow Events. *Frontiers in Marine Science*, *6*(November), 1–18. https://doi.org/10.3389/fmars.2019.00673

Majewski, M. (2001). Water-Quality Monitoring of Sweetwater Reservoir. *USGS Fact Sheet 070-01*. http://pubs.usgs.gov/fs/fs-070-01/fs-070-01.pdf

Manning, A. J., Baugh, J. V., Soulsby, R. L., Spearman, J. R., & Whitehouse, R. J. S. (2011). Cohesive Sediment Flocculation and the Application to Settling Flux Modelling. In *Sediment Transport*. InTech. https://doi.org/10.5772/16055

Mannino, A., & Harvey, H. R. (2000). Terrigenous dissolved organic matter along an estuarine gradient and its flux to the coastal ocean. *Organic Geochemistry*, *31*(12), 1611–1625. https://doi.org/10.1016/S0146-6380(00)00099-1

Mantoura, R., & Woodward, E. M. S. (1983). Conservative behaviour of riverine dissolved organic carbon in the Severn Estuary: chemical and geochemical implications. *Geochimrca et Cosmochimica Acta*, *47*(540), 1293–1309. https://doi.org/10.1016/0016-7037(83)90069-8

Markager, S., Stedmon, C. A., & Søndergaard, M. (2011). Seasonal dynamics and conservative mixing of dissolved organic matter in the temperate eutrophic estuary Horsens Fjord. *Estuarine, Coastal and Shelf Science*, *92*(3), 376–388. https://doi.org/10.1016/j.ecss.2011.01.014

Mayer, L. M. (1982). Aggregation of colloidal iron during estuarine mixing: Kinetics, mechanism, and seasonality. *Geochimica et Cosmochimica Acta*, *46*(12), 2527–2535. https://doi.org/10.1016/0016-7037(82)90375-1

Mayer, L. M., Schick, L. L., Hardy, K. R., & Estapa, M. L. (2009). Photodissolution and other photochemical changes upon irradiation of algal detritus. *Limnology and Oceanography*, *54*(5), 1688–1698. https://doi.org/10.4319/lo.2009.54.5.1688

Meng, S., & Liu, Y. (2016). New insights into transparent exopolymer particles (TEP) formation from precursor materials at various Na + /Ca 2+ ratios. *Scientific Reports*, *6*(January), 1–9. https://doi.org/10.1038/srep19747

Meybeck, M. (1982). Carbon, nitrogen, and phosphorus transport by world rivers. In *American Journal of Science* (Vol. 282, Issue 4, pp. 401–450). https://doi.org/10.2475/ajs.282.4.401

Meyers-Schulte, K. J., & Hedges, J. I. (1986). Molecular evidence for a terrestrial component of organic matter dissolved in ocean water. *Nature*, *321*(6065), 61–63. https://doi.org/10.1038/321061a0

Middelburg, J. J. (2019). Marine Carbon Biogeochemistry A Primer for Earth System Scientists. In *SpringerBriefs in Earth System Sciences*.

Mikkelsen, O. A., Hill, P. S., & Milligan, T. G. (2006). Single-grain, microfloc and macrofloc volume variations observed with a LISST-100 and a digital floc camera. *Journal of Sea Research*, *55*(2), 87–102. https://doi.org/10.1016/j.seares.2005.09.003

Millero, F. J. (2016). *Chemical Oceanography* (4th ed.). CRC Press. https://doi.org/10.1201/b14753

Millward, G. E., & Liu, Y. P. (2003). Modelling metal desorption kinetics in estuaries. *Science of the Total Environment*, *314–316*(January), 613–623. https://doi.org/10.1016/S0048-9697(03)00077-9

Ming, Y., & Gao, L. (2022). Flocculation of suspended particles during estuarine mixing in the Changjiang estuary-East China Sea. *Journal of Marine Systems*, *233*(April), 103766. https://doi.org/10.1016/j.jmarsys.2022.103766

Monbet, Y., Manaud, F., Gentien, P., Pommepuy, M., Allen, G. P., Salomon, J. C., & L'Yavanc, J. (1981). The Use of Nutrients, Salinity and Water Circulation Data as a Tool for Coastal Zone Planning. In *Estuaries and Nutrients* (pp. 343–372). Humana Press. https://doi.org/10.1007/978-1-4612-5826-1_16

Mooney, R. F., & McClelland, J. W. (2012). Watershed export events and ecosystem responses in the Mission–Aransas National Estuarine Research Reserve, South Texas. *Estuaries and Coasts*, *35*(6), 1468–1485. https://doi.org/10.1007/s12237-012-9537-4

Moore, R. M., Burton, J. D., Williams, P. J. LeB., & Young, M. L. (1979). The behaviour of dissolved organic material, iron and manganese in estuarine mixing. *Geochimica et Cosmochimica Acta*, *43*(6), 919–926. https://doi.org/10.1016/0016-7037(79)90229-1

Nayar, S., & Chou, L. M. (2003). Relative efficiencies of different filters in retaining phytoplankton for pigment and productivity studies. *Estuarine, Coastal and Shelf Science*, *58*(2), 241–248. https://doi.org/10.1016/S0272-7714(03)00075-1

Nijssen, B., O'Donnell, G. M., Lettenmaier, D. P., Lohmann, D., & Wood, E. F. (2001). Predicting the Discharge of Global Rivers. *Journal of Climate*, *14*(15), 3307–3323. https://doi.org/10.1175/1520-0442(2001)014%3C3307:PTDOGR%3E2.0.CO;2

Orellana, M. V., Petersen, T. W., Diercks, A. H., Donohoe, S., Verdugo, P., & van den Engh, G. (2007). Marine microgels: Optical and proteomic fingerprints. *Marine Chemistry*, *105*(3–4), 229–239. https://doi.org/10.1016/j.marchem.2007.02.002

Orellana, M. V., & Verdugo, P. (2003). Ultraviolet radiation blocks the organic carbon exchange between the dissolved phase and the gel phase in the ocean. *Limnology and Oceanography*, *48*(4), 1618–1623. https://doi.org/10.4319/lo.2003.48.4.1618

Pancost, R. D., Freeman, K. H., Wakeham, S. G., & Robertson, C. Y. (1997). Controls on carbon isotope fractionation by diatoms in the Peru upwelling region. *Geochimica et Cosmochimica Acta*, *61*(23), 4983–4991. https://doi.org/10.1016/S0016-7037(97)00351-7

Peterson, B. J., & Fry, B. (1987). Stable isotopes in ecosystem studies. *Annual Review of Ecology and Systematics. Vol. 18*, 293–320. https://doi.org/10.1016/0198-0254(88)92720-3

Rabalais, N. N., Díaz, R. J., Levin, L. A., Turner, R. E., Gilbert, D., & Zhang, J. (2010). Dynamics and distribution of natural and human-caused hypoxia. *Biogeosciences*, *7*(2), 585–619. https://doi.org/10.5194/bg-7-585-2010

Rabalais, N. N., & Turner, R. E. (2019). Gulf of Mexico Hypoxia: Past, Present, and Future. *Limnology and Oceanography Bulletin*, *28*(4), 117–124. https://doi.org/10.1002/lob.10351

Rau, G. H., Riebesell, U., & Wolf-Gladrow, D. (1996). A model of photosynthetic 13C fractionation by marine phytoplankton based on diffusive molecular CO2 uptake. *Marine Ecology Progress Series*, *133*(1–3), 275–285. https://doi.org/10.3354/meps133275

Reyna, N. E., Hardison, A. K., & Liu, Z. (2017). Influence of major storm events on the quantity and composition of particulate organic matter and the phytoplankton community in a subtropical Estuary, Texas. *Frontiers in Marine Science*, *4*(FEB). https://doi.org/10.3389/fmars.2017.00043

Rosborg, I., Kozisek, F., & Precautions, S. (2015). Drinking Water Minerals and Mineral Balance. In *Drinking Water Minerals and Mineral Balance*. https://doi.org/10.1007/978-3-319-09593-6

Sampedro-Avila, J. E., Lu, K., Xue, J., Liu, Z., & Maske, H. (2024). The chemical characteristics and mixing behaviors of particulate organic matter from small subtropical rivers in coastal Gulf of Mexico. *Estuarine, Coastal and Shelf Science*, *299*, 108664. https://doi.org/10.1016/j.ecss.2024.108664

Santschi, P. H., Chin, W. C., Quigg, A., Xu, C., Kamalanathan, M., Lin, P., & Shiu, R. F. (2021). Marine gel interactions with hydrophilic and hydrophobic pollutants. *Gels*, *7*(3), 1–14. https://doi.org/10.3390/gels7030083

Schlesinger, W. H., & Melack, J. M. (1981). Transport of organic carbon in the world's rivers. *Tellus*, *33*(2), 172–187. https://doi.org/10.3402/tellusa.v33i2.10706

Schlünz, B., & Schneider, R. R. (2000). Transport of terrestrial organic carbon to the oceans by rivers: re-estimating flux- and burial rates. *International Journal of Earth Sciences*, *88*(4), 599–606. https://doi.org/10.1007/s005310050290

Sholkovitz, E., Boyle, E., & Price, N. (1978). The removal of dissolved humic acids and iron during estuarine mixing. *Earth and Planetary Science Letters*, *40*, 130–136. https://doi.org/10.1016/0272-7714(83)90104-X

Sholkovitz, E. R. (1976). Flocculation of dissolved organic and inorganic matter during the mixing of river water and seawater. *Geochimica et Cosmochimica Acta*, *40*(7), 831–845. https://doi.org/10.1016/0016-7037(76)90035-1

Sholkovitz, E. R., Boyle, E. A., & Price, N. B. (1978). The removal of dissolved humic acids and iron during estuarine mixing. *Earth and Planetary Science Letters*, *40*(1), 130–136. https://doi.org/10.1016/0012-821X(78)90082-1

Sivadon, P., Barnier, C., Urios, L., & Grimaud, R. (2019). Biofilm formation as a microbial strategy to assimilate particulate substrates. *Environmental Microbiology Reports*, *11*(6), 749–764. https://doi.org/10.1111/1758-2229.12785

Smith, B. N., & Epstein, S. (1971). Two Categories of 13C/ 12C Ratios for Higher Plants. *Plant Physiology*, *47*(3), 380–384. https://doi.org/10.1104/pp.47.3.380

Søndergaard, M., Stedmon, C. A., & Borch, N. H. (2003). Fate of terrigenous dissolved organic matter (DOM) in estuaries: Aggregation and bioavailability. *Ophelia*, *57*(3), 161–176. https://doi.org/10.1080/00785236.2003.10409512

Spencer, K. L., Wheatland, J. A. T., Bushby, A. J., Carr, S. J., Droppo, I. G., & Manning, A. J. (2021). A structure–function based approach to floc hierarchy and evidence for the non-fractal nature of natural sediment flocs. *Scientific Reports*, *11*(1), 1–10. https://doi.org/10.1038/s41598-021-93302-9

Sun, L., Chiu, M. H., Xu, C., Lin, P., Schwehr, K. A., Bacosa, H., Kamalanathan, M., Quigg, A., Chin, W. C., & Santschi, P. H. (2018). The effects of sunlight on the composition of exopolymeric substances and subsequent aggregate formation during oil spills. *Marine Chemistry*, *203*(April), 49–54. https://doi.org/10.1016/j.marchem.2018.04.006

Swarzenski, P. W., Campbell, P. L., Osterman, L. E., & Poore, R. Z. (2008). A 1000-year sediment record of recurring hypoxia off the Mississippi River: The potential role of terrestrially-derived organic matter inputs. *Marine Chemistry*, *109*(1–2), 130–142. https://doi.org/10.1016/j.marchem.2008.01.003

Swarzenski, P. W., Porcelli, D., Andersson, P. S., & Smoak, J. M. (2003). The behavior of U- and Th-series nuclides in the estuarine environment. *Uranium-Series Geochemistry*, *52*(Fairbridge), 577–606. https://doi.org/10.2113/0520577

Synek, V. (2008). Evaluation of the standard deviation from duplicate results. *Accreditation and Quality Assurance*, *13*(6), 335–337. https://doi.org/10.1007/s00769-008-0390-x

Tang, D., Warnken, K. W., & Santschi, P. H. (2002). Distribution and partitioning of trace metals (Cd, Cu, Ni, Pb, Zn) in Galveston Bay waters. *Marine Chemistry*, *78*(1), 29–45. https://doi.org/10.1016/S0304-4203(02)00007-5

Thurman, E. M. (1985). Organic Geochemistry of Natural Waters. In *Geochimica et Cosmochimica Acta* (Vol. 50, Issue 9). Springer Netherlands. https://doi.org/10.1007/978-94-009-5095-5

Valdés-Villaverde, P. J. (2018). *Exploración metodológica del potencial de formación de geles marinos*. [Master in Science Thesis, Centro de Investigación Científica y de Educación Superior de Ensenada, Baja California]. https://cicese.repositorioinstitucional.mx/jspui/handle/1007/2779

Valikhani Samani, A. R., Karbassi, A. R., Fakhraee, M., Heidari, M., Vaezi, A. R., & Valikhani, Z. (2015). Effect of dissolved organic carbon and salinity on flocculation process of heavy metals during mixing of the Navrud River water with Caspian Seawater. *Desalination and Water Treatment*, *55*(4), 926–934. https://doi.org/10.1080/19443994.2014.920730

Van Vliet, M. T. H., Franssen, W. H. P., Yearsley, J. R., Ludwig, F., Haddeland, I., Lettenmaier, D. P., & Kabat, P. (2013). Global river discharge and water temperature under climate change. *Global Environmental Change*, *23*(2), 450–464. https://doi.org/10.1016/j.gloenvcha.2012.11.002

Vaquer-Sunyer, R., & Duarte, C. M. (2008). Thresholds of hypoxia for marine biodiversity. *Proceedings of the National Academy of Sciences of the United States of America*, *105*(40), 15452–15457. https://doi.org/10.1073/pnas.0803833105

Verdugo, P. (2012). Marine Microgels. *Annual Review of Marine Science*, *4*(1), 375–400. https://doi.org/10.1146/annurev-marine-120709-142759

Verdugo, P., Orellana, M. V., Chin, W. C., Petersen, T. W., Van Den Eng, G., Benner, R., & Hedges, J. I. (2008). Marine biopolymer self-assembly: Implications for carbon cycling in the ocean. *Faraday Discussions*, *139*, 393–398. https://doi.org/10.1039/b800149a

Wang, Y., & Gao, L. (2022). Sources and dynamics of suspended particulate matter in a large-river dominated marine system: Contributions from terrestrial sediments, biological particles, and flocculation. *Journal of Marine Systems*, *225*(October 2021), 103648. https://doi.org/10.1016/j.jmarsys.2021.103648

Wangersky, P. J. (1984). Organic Particles and Bacteria in the Ocean. In *Heterotrophic Activity in the Sea* (Vol. 34, Issue 11, pp. 263–288). Springer US. https://doi.org/10.1007/978-1-4684-9010-7_13

Wei, H., Xu, X., Jones, A. E., Hardison, A. K., Moffett, K. B., & McClelland, J. W. (2022). Tidal Freshwater Zones Modify the Forms and Timing of Nitrogen Export from Rivers to Estuaries. *Estuaries and Coasts*, *45*(8), 2414–2427. https://doi.org/10.1007/s12237-022-01112-7

Wei, H., Xu, X., Savoie, A., Schattle, E., Hardison, A. K., Erdner, D. L., & McClelland, J. W. (2023). Seasonal and nutrient controls on phytoplankton in the Aransas River tidal freshwater zone, Texas, USA. *Hydrobiologia*, *0123456789*. https://doi.org/10.1007/s10750-023-05388-z

Wickham, H., Averick, M., Bryan, J., Chang, W., McGowan, L., François, R., Grolemund, G., Hayes, A., Henry, L., Hester, J., Kuhn, M., Pedersen, T., Miller, E., Bache, S., Müller, K., Ooms, J., Robinson, D., Seidel, D., Spinu, V., … Yutani, H. (2019). Welcome to the Tidyverse. *Journal of Open Source Software*, *4*(43), 1686. https://doi.org/10.21105/joss.01686

Woebken, D., Fuchs, B. M., Kuypers, M. M. M., & Amann, R. (2007). Potential interactions of particle-associated anammox bacteria with bacterial and archaeal partners in the Namibian upwelling system. *Applied and Environmental Microbiology*, *73*(14), 4648–4657. https://doi.org/10.1128/AEM.02774-06

Wu, K., Lu, K., Dai, M., & Liu, Z. (2019). The bioavailability of riverine dissolved organic matter in coastal marine waters of southern Texas. *Estuarine, Coastal and Shelf Science*, *231*(November), 106477. https://doi.org/10.1016/j.ecss.2019.106477

Xu, C., Chin, W. C., Lin, P., Chen, H., Chiu, M. H., Waggoner, D. C., Xing, W., Sun, L., Schwehr, K. A., Hatcher, P. G., Quigg, A., & Santschi, P. H. (2019). Comparison of microgels, extracellular polymeric substances (EPS) and transparent exopolymeric particles (TEP) determined in seawater with and without oil. *Marine Chemistry*, *215*(June), 103667. https://doi.org/10.1016/j.marchem.2019.103667

Xu, X., Wei, H., Barker, G., Holt, K., Julian, S., Light, T., Melton, S., Salamanca, A., Moffett, K. B., McClelland, J. W., & Hardison, A. K. (2021). Tidal Freshwater Zones as Hotspots for Biogeochemical Cycling: Sediment Organic Matter Decomposition in the Lower Reaches of Two South Texas Rivers. *Estuaries and Coasts*, *44*(3), 722–733. https://doi.org/10.1007/s12237-020-00791-4

Zajączkowski, M. (2008). Sediment supply and fluxes in glacial and outwash fjords: Kongsfjorden and Adventfjorden, Svalbard. *Polish Polar Research*, *29*(January 2008), 59–72.

Supplementary material

S.1. Calculation of mixing lines for POC/PON, POC-δ13C, PON-δ15N, and THAA-C/POC

Conservative mixing lines for these parameters were calculated with RStudio software (version 2022.07.2+576), using R base functions. The following equations were used for each parameter.

POC/PON was represented by *f(s)* at each studied salinity, to calculate the conservative mixing line (Equation S1):

$$f(S) = \frac{POC_{SW} + (POC_{RW} - POC_{SW}) \cdot \frac{Salin_{SW} - S}{Salin_{SW} - Salin_{RW}}}{PON_{SW} + (PON_{RW} - PON_{SW}) \cdot \frac{Salin_{SW} - S}{Salin_{SW} - Salin_{RW}}}$$

Where *S* is the salinity in the mixed water, POC_{SW} and POC_{RW} are the POC values measured in the seawater and river water end members, respectively, and PON_{SW} and PON_{RW} are the PON values measured in the same end members, respectively. $Salin_{SW}$ and $Salin_{RW}$ are the salinity values in the seawater and the river water, respectively.

POC-δ^{13}C was represented by *f(s)* at each studied salinity, to calculate the conservative mixing line (Equation S2):

$$f(S) = \left[\frac{\left(\frac{^{13}C_{SW} + (^{13}C_{RW} - ^{13}C_{SW}) \cdot \frac{Salin_{SW} - S}{Salin_{SW} - Salin_{RW}}}{^{12}C_{SW} + (^{12}C_{RW} - ^{12}C_{SW}) \cdot \frac{Salin_{SW} - S}{Salin_{SW} - Salin_{RW}}} \right)}{\frac{^{13}C}{^{12}C}_{VPDB}} - 1 \right] \cdot 1000$$

Where *S* is the salinity in the mixed water, $^{13}C_{SW}$ and $^{13}C_{RW}$ are the ^{13}C values calculated from the POC-δ^{13}C measured in the seawater and river water end members, respectively, and $^{12}C_{SW}$ and $^{12}C_{RW}$ are the ^{12}C values from the POC-δ^{13}C measured in the same end members, respectively. $Salin_{SW}$ and $Salin_{RW}$ are the

salinity values in the seawater and the river water, respectively. $^{13}C/^{12}C_{VPDB}$ is the "Vienna Pee Dee Belemnite" standard value (0.01123720).

PON-$\delta^{15}N$ was represented by *f(s)* at each studied salinity, to calculate the conservative mixing line (Equation S3):

$$f(S) = \left[\frac{\left(\frac{^{15}N_{SW} + (^{15}N_{RW} - {}^{15}N_{SW}) \cdot \frac{Salin_{SW} - S}{Salin_{SW} - Salin_{RW}}}{^{14}N_{SW} + (^{14}N_{RW} - {}^{14}N_{SW}) \cdot \frac{Salin_{SW} - S}{Salin_{SW} - Salin_{RW}}} \right)}{\frac{^{15}N}{^{14}N_{AIR}}} - 1 \right] \cdot 1000$$

Where *S* is the salinity in the mixed water, $^{15}N_{SW}$ and $^{15}N_{RW}$ are the ^{15}N values calculated from the PON-$\delta^{15}N$ measured in the seawater and river water end members, respectively, and $^{14}N_{SW}$ and $^{14}N_{RW}$ are the ^{14}N values from the PON-$\delta^{15}C$ measured in the same end members, respectively. $Salin_{SW}$ and $Salin_{RW}$ are the salinity values in the seawater and the river water, respectively. $^{15}N/^{14}N_{AIR}$ is the air standard value (0.003676).

THAA-C/POC was represented by *f(S)* at each studied salinity, to calculate the conservative mixing line (Equation S4):

$$f(S) = \frac{THAAC_{SW} + (THAAC_{RW} - THAAC_{SW}) \cdot \frac{Salin_{SW} - S}{Salin_{SW} - Salin_{RW}}}{POC_{SW} + (POC_{RW} - POC_{SW}) \cdot \frac{Salin_{SW} - S}{Salin_{SW} - Salin_{RW}}}$$

Where *S* is the salinity in the mixed water, $THAAC_{SW}$ and $THAAC_{RW}$ are the carbon content values which were stoichiometrically calculated from the total hydrolyzable amino acids (THAA) measured in the seawater and river water end members, respectively. PON_{SW} and PON_{RW} are the PON values measured in the same end members, respectively. $Salin_{SW}$ and $Salin_{RW}$ are the salinity values in the seawater and the river water, respectively.

S.2. Bulk particulate organic matter in the Trinity, Neches and Atchafalaya Rivers experiments.

Additional experiments with water from Trinity, Neches and Atchafalaya rivers (Fig. S1) were conducted in a same way as the Mission and Aransas rivers. However, only one mixing proportion was prepared for each river experiment (corresponding to 20% seawater + 80% river water in the Trinity and Atchafalaya experiments, and 10% seawater + 90% river water in the Neches River experiment), besides of the two end members.

Particulate organic carbon (POC; Fig. S2a) and nitrogen (PON; Fig. S2b) were measured and POC/PON ratio was calculated (Fig. S2c). Other parameters were measured in the river and seawater endmembers (Table S1).

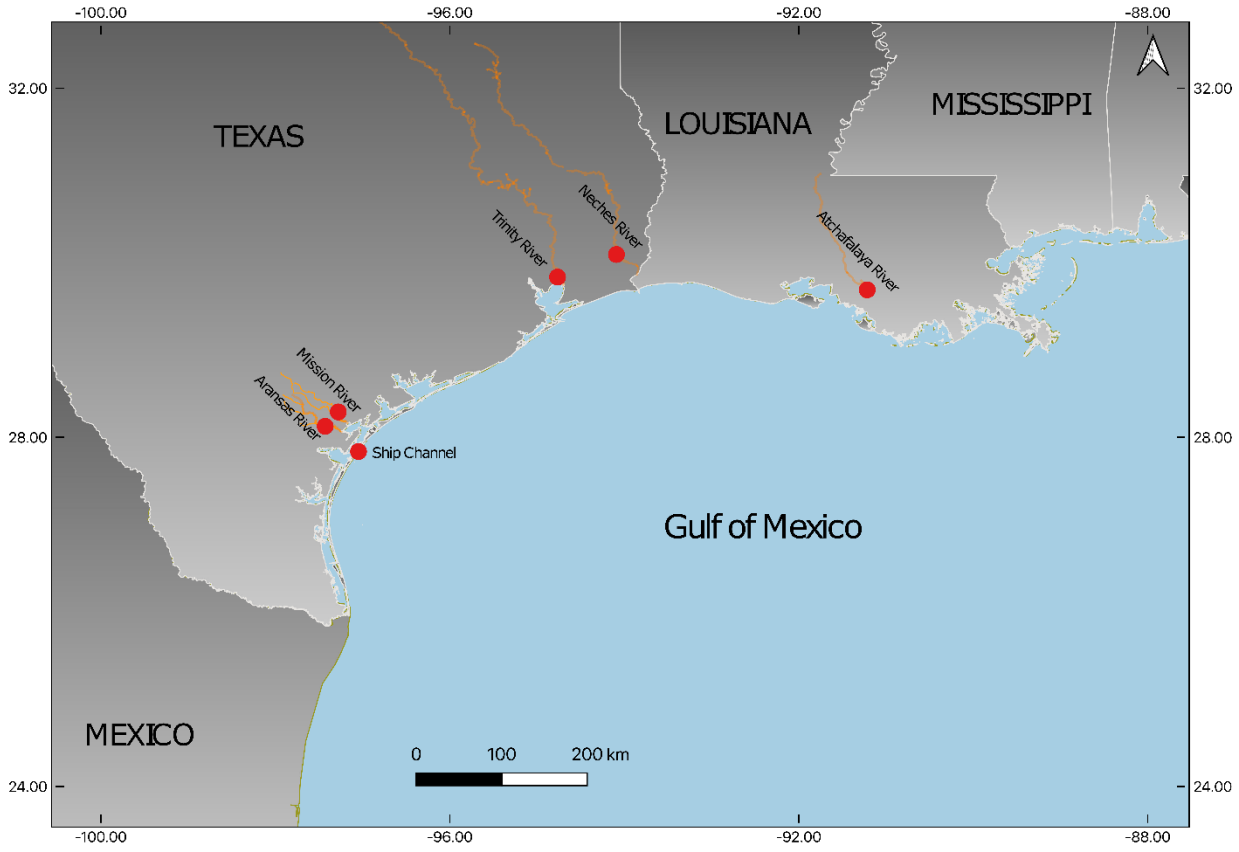

Figure 19. Sampling locations for the Atchafalaya River, the Neches River, the Trinity River, the Mission River, the Aransas River, and the Port Aransas Ship Channel.

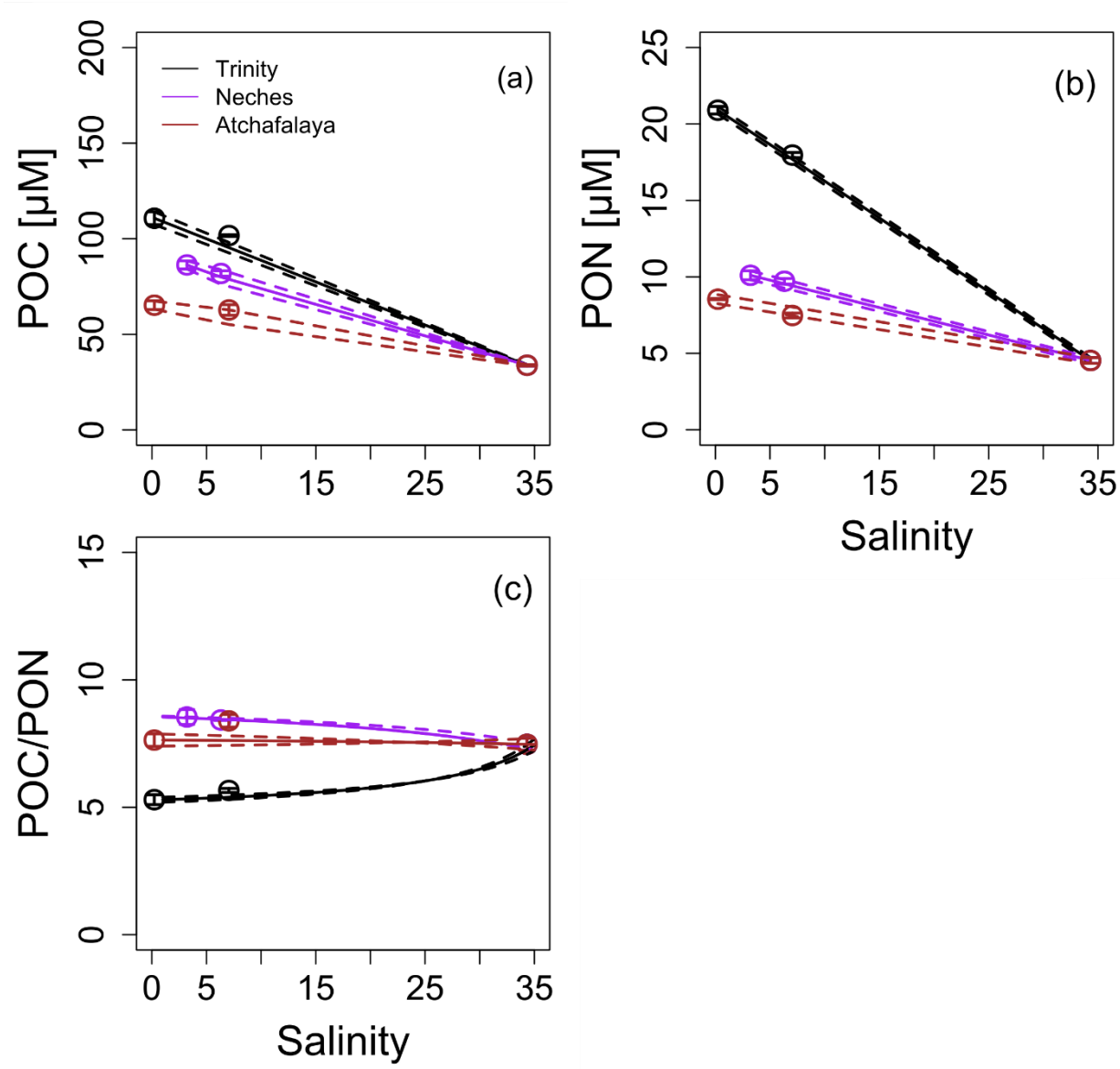

Figure 20. Bulk particulate organic carbon (POC; a), particulate organic nitrogen (PON; b), and POC/PON ratio (c), from laboratory experiments with Trinity, Neches, and Atchafalaya Rivers, all mixed with seawater in each experiment. Mean values from experimental treatments are represented with black (Trinity), purple (Neches) and brown (Atchafalaya) circles. Conservative mixing lines calculated from end members are solid. Dotted lines and error bars represent the standard deviation (n=3).

Table 3. Hydrographic conditions, sampling coordinates in the Trinity, Neches and Atchafalaya rivers, and the different parameters measured in these experiments.

	Trinity River	**Neches River**	**Atchafalaya River**
Latitude (°N)	29.84	30.09	29.69
Longitude (°E)	-94.76	-94.09	-91.21
Hardness (mg $CaCO_3L^{-1}$)	77	354	89
Salinity	0.23	3.21	0.23
pH	8.1	7.72	7.89
DO (mg L^{-1})	11.21	16.28	13.19
POC [µM]	111	86	65
PON [µM]	21	10	9
POC/PON	5.3	8.5	7.6
δ^{13}C-POC (‰)	-32.3	-30.9	-30.4
δ^{15}N-PON (‰)	8.4	4.4	10.1
PIC [µM]	25	10	0
DOC [µM]	401	538	262
DON [µM]	24	17	16
DOC/DON	17	31	16
DIN [µM]	4	10	30

S.3. Nitrogen isotopic signature (δ^{15}N-PON) in the Mission and Aransas Rivers experiments.

δ^{15}N-PON values were measured with an elemental analyzer as explained in section 2.3 ("Elemental composition and stable isotopes analysis") and conservative mixing lines were calculated as explained in section 1 ("Calculation of mixing lines for POC/PON, POC-δ^{13}C, PON-δ^{15}N, and THAA-C/POC", supplementary material). The original mixing curve measured for the Mission River 2022 experiment (data not shown) was optimized with an $^{15}N/^{14}N$ ratio of 0.00372976 in the riverine end member, to obtain the best fit to the measured data averages (R^2 = 0.85).

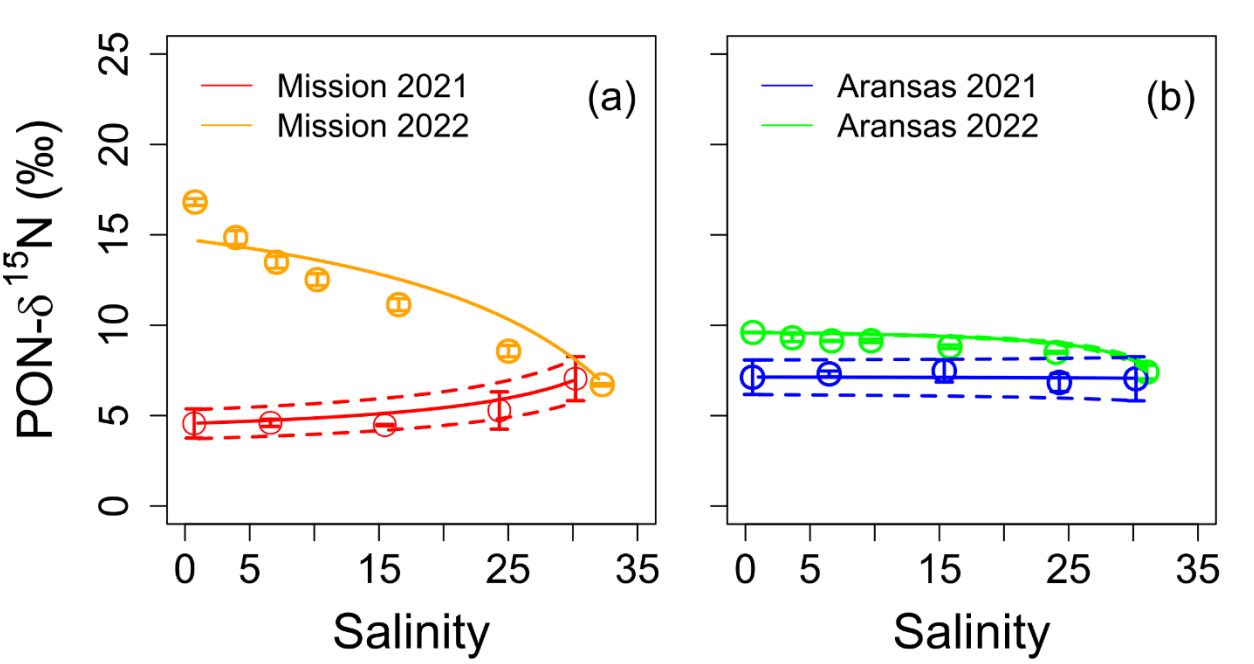

Figure 21. Bulk particulate organic δ15N (POC-δ15N) from laboratory experiments with Mission River (a) and Aransas River (b) water, both mixed with seawater at different proportions. Mean values from experimental treatments with Mission River water are represented with red (2021) and orange (2022) circles, and data from Aransas River water is in blue (2021) and green (2022). Conservative mixing lines calculated from end members are solid. Dotted lines and error bars represent the standard deviation (n=2 in 2021 and n=3 in 2022 experiments).

S.4. Amino acids composition in the Mission and Aransas Rivers experiments

Principal component analysis (PCA) suggested different particulate amino acids composition (mol%) between the Mission River and the Aransas River experiments in 2022 (Fig. S4; confidence interval = 95%). The Aransas River (2022) was enriched in glutamic acid (GLU), while the Mission River (2022) was enriched in its degradation product GABA. Other PCAs were performed to compare experiments but no significant differences were observed.

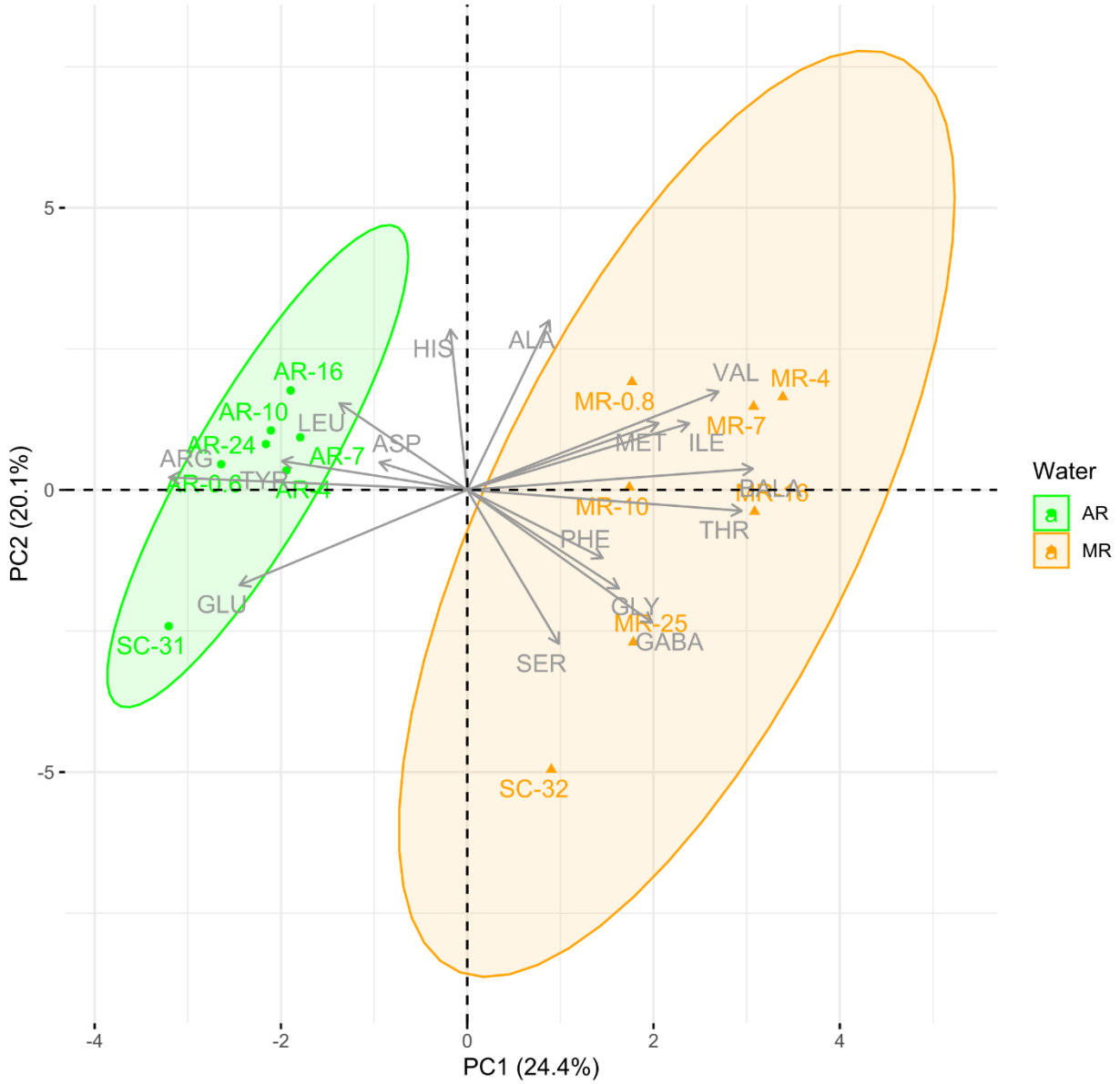

Figure 22. PCA of hydrolyzable amino acids mol percentage from the experiments of mixed water from the Mission River and the Aransas River with seawater in 2022. Ellipses represent the confidence interval (95%).

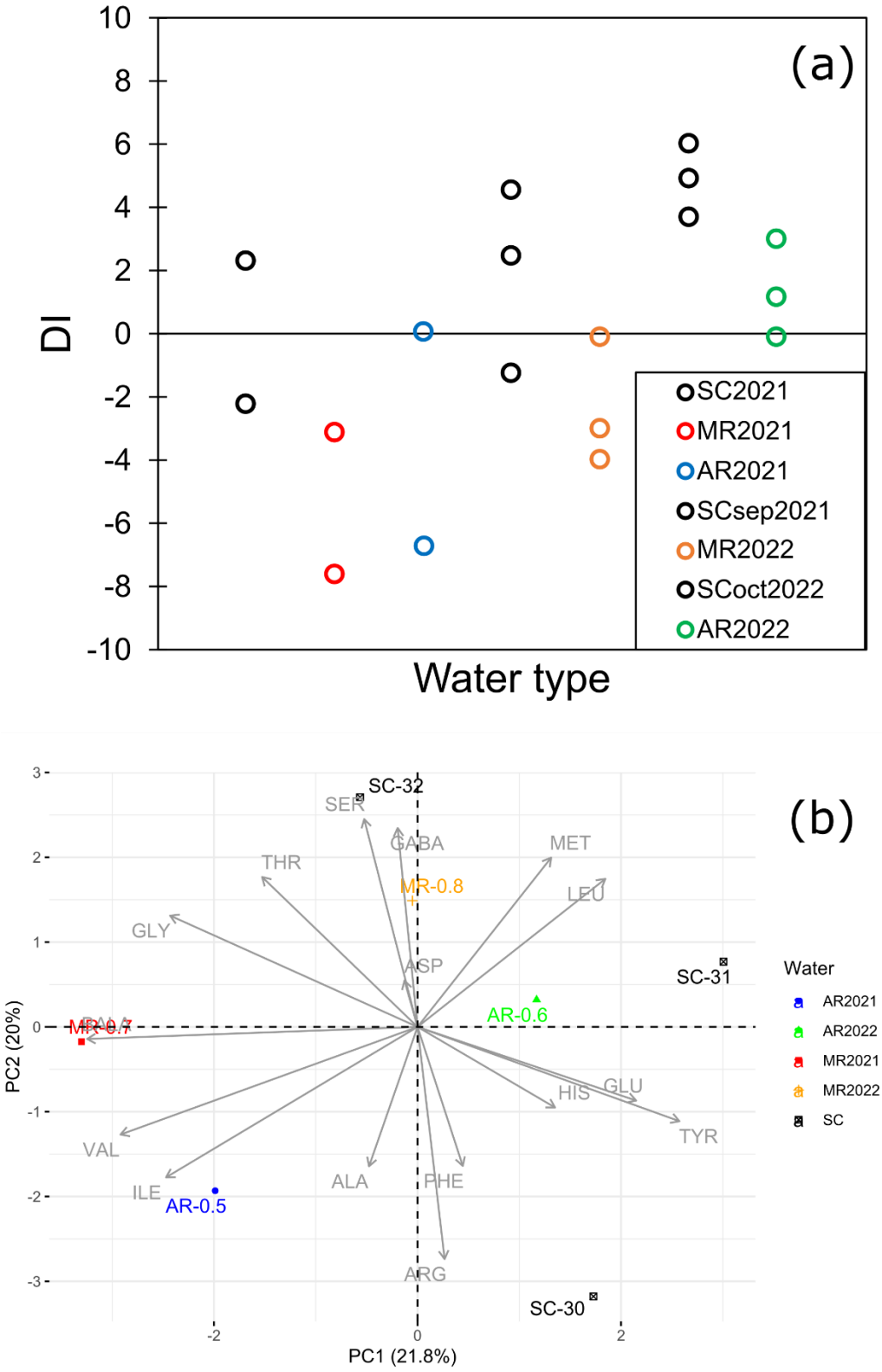

Figure 23. Degradation index (a) calculated from a PCA of the hydrolyzable amino acids from end members of mixing experiments conducted with seawater and river water from the Mission and Aransas rivers in 2021 and 2022 (b).

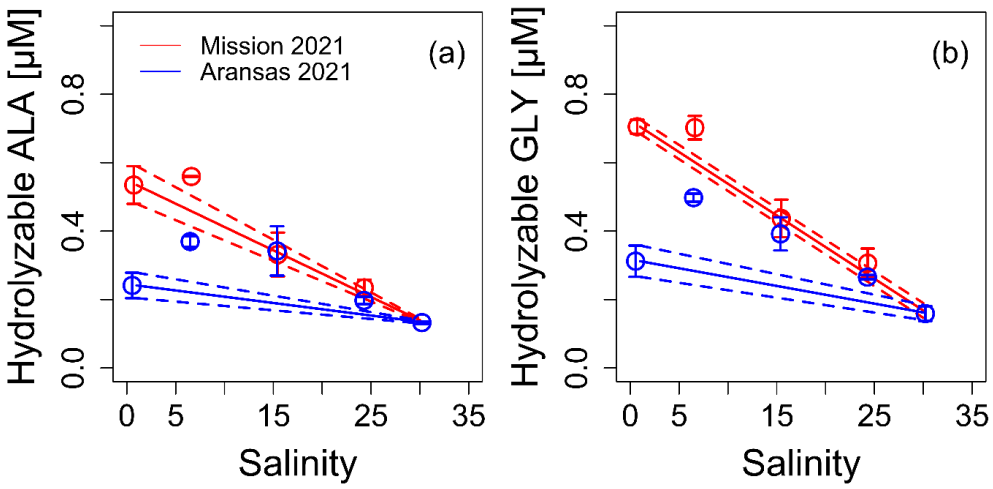

Figure 24. Hydrolyzable alanine (ALA; a) and glycine (GLY; b) concentrations from laboratory experiments with Mission River and Aransas River (Texas) water, both mixed with seawater at different proportions. Mean values from experimental treatments with Mission River water are represented with red (2021), and data from Aransas River water are in blue (2021).

GLY (Glycine) and Alanine (ALA) were the most abundant (18 and 13%, respectively) from the total hydrolyzable amino acids (THAA) in all experiments. These two amino acids were higher than the mixing line in the Aransas River experiment from 2021 (Fig. S6), coinciding with the observed THAA increase (Fig. 3d). Degradation indexes were calculated (Fig. S5a) from a PCA with end members from all the experiments conducted with the Mission and the Aransas rivers (Fig. S5b). The DI of the Aransas River water from 2022 was higher than the Mission River from 2021 ($p = 0.03$).

S.5. Satellite images results presented in Sampedro-Avila et al. (2020, Ocean Science Meeting) to observe POM formation associated to rainfall in the Southern Gulf of Mexico

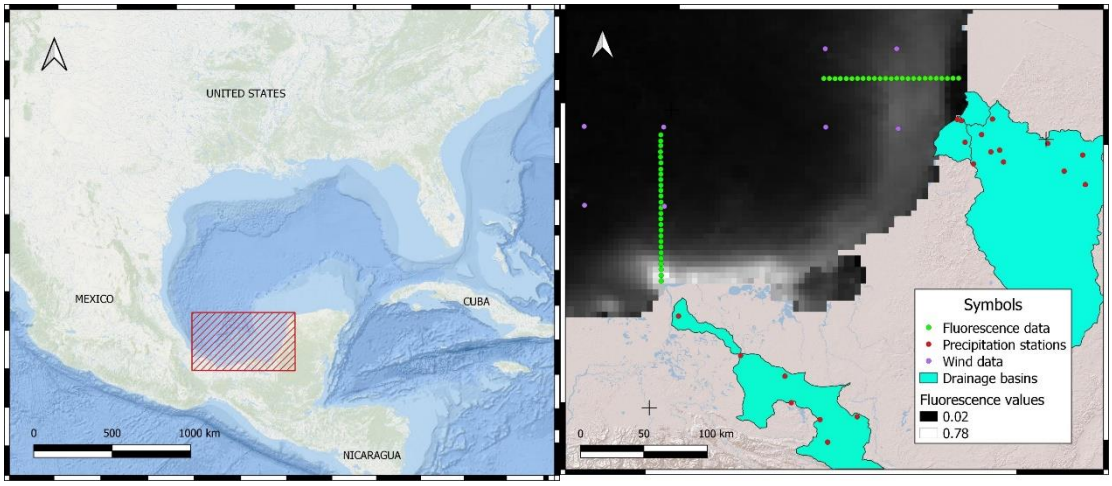

Figure 25. Location of satellite images analyzed for normalized fluorescence line height), and winds (nFLH, MODIS-Aqua), and precipitation stations.

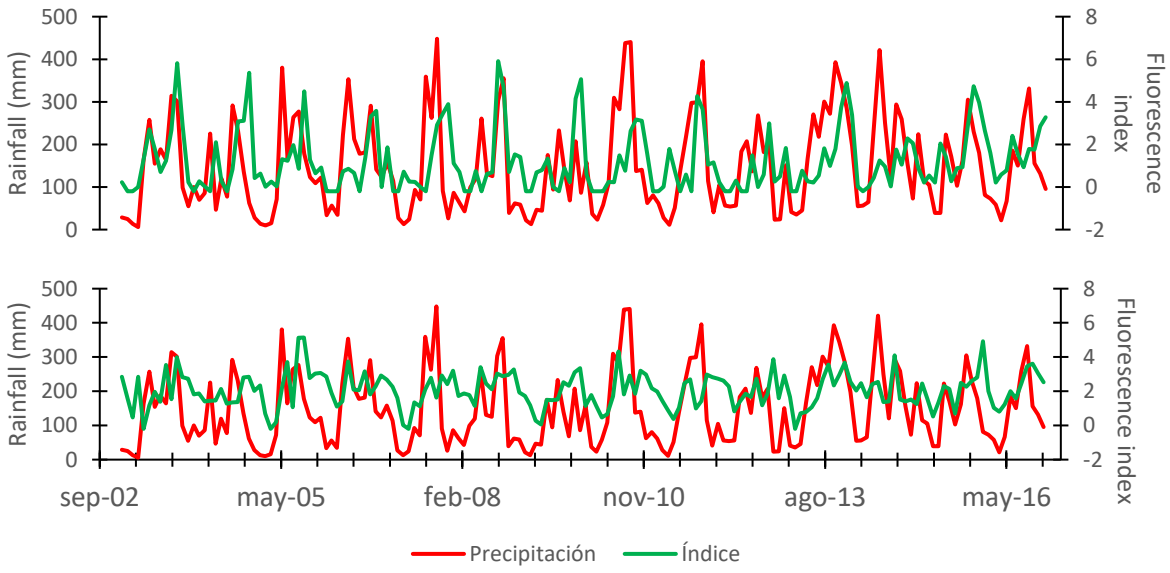

Figure 26. Fluorescence (MODIS-Aqua) and rainfall (CONAGUA) time series correlation (2003-2016). The green line represents the fluorescence index, and the red line represents the monthly accumulated rainfall.